Abstract Volume
11th Swiss Geoscience Meeting

Lausanne, 15th – 16th November 2013

1. Structural Geology, Tectonics and Geodynamics

sc | nat

Swiss Academy of Sciences
Akademie der Naturwissenschaften
Accademia di scienze naturali
Académie des sciences naturelles

UNIL | Université de Lausanne
Faculté des géosciences
et de l'environnement

1. Structural Geology, Tectonics and Geodynamics

Neil Mancktelow, Guido Schreurs, Paul Tackley

Swiss Tectonics Studies Group of the Swiss Geological Society

TALKS:

1.1 Houlie N., Stern T.: A comparison of GPS solutions for strain and SKS fast directions: implications for modes of shear in the mantle of a plate boundary zone

1.2 Hunziker D., Burg J.-P., Vonquadt A., Bouilhol P.: Jurassic extension in Northern Makran, SE Iran: Geochemistry, U/Pb ages and Sr-Nd isotopes

1.3 Kaczmarek M.-A., Grange M., Reddy S.M., Nemchin A.: Deformation mechanisms in Martian meteorites

1.4 Lourenço D. L. , Tackley P. J.: The effect of melting and crustal production on plate tectonics on terrestrial planets

1.5 Malz A., Madritsch H., Meier B., Navabpour P., Heuberger S., Kley J.: The Baden-Irchel-Herdern Lineament: An inherited normal fault controlling the front of the eastern Jura fold-and-thrust belt

1.6 Moulas E., Burg J-P., Podladchikov Y.: Rheology-driven phase equilibria and the in-situ formation of high-pressure rocks

1.7 Nazari H., Ghorashi M., Kaveh Firouz A.: Probable Tsunami In The South Caspian Sea By A Large Earthquake!

1.8 Sala P., Pfiffner A.: The internal structure of the Säntis nappe: folds, thrusts and wrench faults

1.9 Schubert R., Herwegh M.: Kinematics and 3D pattern of ductile shear zones in the Gruebensee-Gelmersee transect (Hasli Valley, central Switzerland).

1.10 Simon-Labric T., Reiners P., Braun J.: Orographic precipitations need glaciers to control long-term erosion rates and topography of tectonically inactive mountain ranges

1.11 Strasser, M., Kodaira, S., Dinten, D.: Structural and morphoplogical changes in the shallow plate boundary system and trench, triggered by rare subduction megathrust earthquakes

1.12 Valla P.G., Rahn M., Shuster D.L., van der Beek P.A.: Exhumation history, topographic relief evolution and geothermal activity in the Swiss Central Alps (Rhône valley): insights from low-temperature thermochronology

1.13 Wehrens P., Herwegh M., Berger A.: Fluid involved, high grade cataclasis during Alpine ductile deformation in basement rocks of the Aar massif

POSTERS:

P 1.1 Bagheri S., Sarani M.: On the origin of the Naybandan Arc-shaped structures, Tabas, Central Iran

P 1.2 Bauville A., Schamlholz S.M.: 2D thermo-mechanical modeling of basement-cover deformation with application to the Western Alps

P 1.3 Buchs D., Cukur D., Masago H.: Tectonosedimentary evolution of the Nankai forearc (Japan) constrained by detrital minerals in off-shore (IODP) drill sites and modern river beds

P 1.4 Cioldi S., Moulas E., Burg J.P.: Geospeedometry of inverted metamorphic gradients of a crustal-scale thrust zone: first approach

P 1.5 Collignon M., May D. A., Kaus B. J.P., Fernandez N.: Effects of surface processes on multilayer detachment folding: a numerical approach.

P 1.6 Duretz T., Schmalholz S. M.: Thermo-mechanical feedback and modelling of crustal-scale shear zones

P 1.7 Fischer R., Gerya T.: Was plate tectonics different in a hotter Earth? History and evolution of subduction in the Precambrium

P 1.8 Frehner M.: 3D fold growth rates

P 1.9 Golabek G., Jutzi M., Gerya T., Asphaug E.: Towards coupled giant impact and long term interior evolution models

P 1.10 Gruber M., Sommaruga A., Mosar J.: 3D Modeling of the Fribourg Area - Western Swiss Molasse Basin, Switzerland

P 1.11 Jaquet Y., Bauville A., Schmalholz S.: Viscous overthrusting versus folding: 2-D quantitative modeling and its application to the Helvetic and Jura fold and thrust belts

P 1.12 Kelevitz K., Houlie N., Rothacher M., Giardini D.: Mapping Earth's interiors with GPS records: the first steps.

P 1.13 Kilian R.: The role of phase distribution and reaction in an amphibolite facies ultramylonite

P 1.14 Liao J., Gerya T.: Offsetting crustal and mantle neckings generates abandonment of continental rifts

P 1.15 Lupi, M., Miller, S. A.: Deformation of the Sumatran, Chilean, and Japanes volcanic arcs after mega-thrust slips.

P 1.16 Malz A., Jordan P., Meier B., Madritsch H., Navabpour P., Kley J.: Tectonic events predating the formation of the Jura fold-and-thrust belt: Constraints from cross section balancing

P 1.17 Marti S., Heilbronner R., Stünitz H.: Semi-brittle deformation of fault rocks - an experimental study of the brittle-to-viscous transition in mafic rocks

P 1.18 May D. A.: A scalable, parallel matrix-free Stokes solver for geodynamics applications

P 1.19 Mohammadi A., Winkler W., Burg J.P., Ruh J., Von Quadt A.: Detrital zircon and provenance analysis on the onshore Makran accretionary wedge, SE Iran: implication for the geodynamic setting

P 1.20 Moulas E., Burg J-P., Kostopoulos D., Schenker F., Chatzitheodoridis E.: Metamorphic conditions and exhumation of the Keshebir-Kardamos dome – Rhodope Metamorphic Complex (Greece-Bulgaria)

P 1.21 Niane B., Moritz R., Guédron S., Poté J., Ngom P M., Pfeifer H.-R.: Assessment of mercury distribution in sediments, soil, fish and human hair sampled in gold mining areas in the Gambia River Basin at Kedougou, southeastern Senegal

P 1.22 Philippe T.A., Frehner M., May D.A.: Single Viscous Layer Fold Interplay And Linkage: A 3d-Fem Modelling Approach

P 1.23 Rabin M., Sue C., Champagnac J.D. & Eichenberger U.: Geomorphology approach in karstic domain: importance of underground water.

P 1.24 Richter B., Kilian R., Stünitz H., Heilbronner R.: The effect of hot-pressing on the grain size distribution and microstructure of quartz gouge along the brittle-to-viscous transition in shear experiments

P 1.25 Rozel A., Tackley P.J.: Convection and grain size evolution in mantle and lithosphere of the Earth

P 1.26 Schmalholz S.M., Medvedev S., Lechmann S.M., Podladchikov Y.: Relationship between tectonic overpressure, deviatoric stress, driving force, isostasy and gravitational potential energy

P 1.27 Valla P.G., Lowick S.E., Herman F., Champagnac J.-D., Guralnik B., Steer P., Chen J., Qin J.: Exploring feldspar IRSL-50 as a low-temperature thermochronometer: insights from field applications (Alaska, Norway and Pamir)

P 1.28 Von Tscharner, M., Schmalholz, S.: 3D FEM modelling of geological structures caused by geometrical instabilities and contrasts in rock strength

P 1.29 Von Tscharner, M., Duretz, T., Schmalholz, S.: Slab detachment – 3D versus 1D

P 1.30 Zhu Y.F.: Baijiantan-Baikouquan ophiolitic mélanges: Implications for geology evolution of west Junggar, Xinjiang, NW China

1.1

A comparison of GPS solutions for strain and SKS fast directions: implications for modes of shear in the mantle of a plate boundary zone

By Houlié N. and Stern, T.

Institut für Geodäsie und Photogrammetrie, IGP, ETH Zürich

The strain rate and vertical velocity fields for New Zealand are computed using GPS data from GEONET (NZ) collected during the past decade. Two domains for shear in the mantle are inferred by comparing the principal shortening direction with the fast direction of shear wave splitting. Beneath the central-southern part of the South Island the strains are low and it's unclear if irrotational strain is taking place or if the splitting here is dominated by anisotropy in the asthenosphere. In contrast, data for the central and northern South Island suggest simple shear is dominant and distributed over a zone ~ 200 km wide. An analysis of the major strike-slip faults confirms that the strike of the major South Island fault systems makes a 60 +- 15$ degree angle with the shortening direction. A map of the vertical component of GEONET GPS velocities shows regions of surface uplift > 5mm/y in both the central South and North Islands. While the pattern of uplift in central South Island is consistent with known geology, the rate of uplift in the central North Island is an order of magnitude higher than the geological rate estimated on a my time scale.

1.2

Jurassic extension in Northern Makran, SE Iran: Geochemistry, U/Pb ages and Sr-Nd isotopes

Hunziker Daniela[1], Burg Jean-Pierre [1], Von Quadt Albrecht[2], Bouilhol Pierre[3]

[1] *Strukturgeologie und Tektonik, Geologisches Institut, ETH Zürich, Sonneggstrasse 5, CH-8092 Zürich (daniela.hunziker@erdw.ethz.ch)*
[2] *Institut für Geochemie und Petrologie, Clausiusstrasse 25, 8092 Zürich*
[3] *Department of Earth Sciences, Durham University*

We present major and trace element analyses combined with U-Pb zircon crystallization ages from an intermediate to granitic intrusion sequence within the Dur Kan Complex, in the Iranian North Makran. The sampled granites – diorites – trondhjemites – plagiogranites and basaltic to andesitic lavas have tholeiitic and calc-alkaline chemical features. Field observations, petrographic relationships, trace element compositions and isotope chemistry indicate three different melt sources for granites, granitoids and the volcanic rocks. Granites yield 170-175Ma ages and represent the last crystallized melt of a continentally derived magma. The fractional crystallization dominated diorite-trondhjemite-plagiogranite sequence was crystallizing over 12Ma (165-153Ma) from the same source which has a mantle and minor continental component. East-west trending mafic dykes intruded the granitoids, which were eroded before being covered by lavas and their Cretaceous (Valangian) sedimentary cover. The source of dykes and lavas is mantle derived.

Temporal correlation with plutonites from the Sanandaj-Sirjan Zone suggests a narrow northwest-southeast striking belt of Jurassic granitoid intrusions that extends over nearly 2000km. Different than previous studies in the Sanandaj-Sirjan Zone, that interpreted these rocks as a magmatic arc and proof for Jurassic subduction of the Neotethys, we suggest extension, that separated the Sanandaj-Sirjan Zone and Central Iran. The increasing mantle influence in the magma source is explained by continuous thinning of continental crust and related mantle up-welling. This extensional phase resulted in the formation of the North Makran Ophiolites.

1.3

Deformation mechanisms in Martian meteorites

Kaczmarek Mary-Alix[1], [2], Grange Marion[2], Reddy Steve M.[2], Nemchin Alexander[2]

[1] *University of Lausanne, Institute of Earth Science, UNIL Mouline, Batiment Geopolis, CH-1016 Lausanne, Switzerland (mary-alix.kaczmarek@unil.ch)*
[2] *Department of Applied Geology, The Institute for Geoscience Research, Curtin University of Technology, GPO Box U1987, Perth, WA 6845, Australia*

Martian meteorites are used to decipher the deformation mechanisms that have occurred on Mars before excavation of the rocks and during shock event(s). Quantitative microstructural analysis of minerals using Electron Backscatter Diffraction (EBSD), and geochemistry are combined to characterise processes recorded by sub-samples of both Nakhla and Zagami meteorites.

Nakhla and Zagami are clinopyroxene-rich basaltic meteorites, and Nakhla contains some Fe-rich olivine. Nakhla displays a granular texture, essentially composed of augite, fayalite, plagioclase and magnetite. The Zagami sample, essentially formed by clinopyroxene, plagioclase transformed in maskelynite, and whitlockite is part of the "coarse grained" portion of Normal Zagami texture (Stolper et al. 1979; McCoy et al. 1992). The sample shows long prisms of clinopyroxene underlying a weak preferrential orientation. The chemical composition of clinopyroxenes reveals zoning from augite cores to pigeonite rims in both samples. However, chemcial zoning in Zagami clinopyroxenes is more complex than in Nakhla and suggests melt interactions. In Nakhla the Mg# of olivine (between 0.30 and 0.32) is in equilibrium with Mg# of clinopyroxene rims (0.31) suggesting a late crystallization of olivine.

Crystallographic orientation data from whole thin section of both Zagami and Nakhla samples show a preferred orientation of clinopyroxene and CPOs displaying several point concentrations of <001> axes within a girdle. The relationship between the microstructure and CPOs inferred the possible activation of (100)[001] and (010)[100] slip systems in clinopyroxenes. Moreover, the crystallographic orientations of olivine grains in Nakhla are random and discordant to clinopyroxene. This is in accordance to a late crystallization of olivine in a cumulate texture. The several point concentrations on clinopyroxene <001> axis correspond to twinning along (100), (001) or (010) planes. Microstructural analysis of clinopyroxene single grains show that Nakhla clinopyroxenes have almost no internal deformation, whilst Zagami clinopyroxenes showing complicated microtextures with possible activation of several slip systems related to the shock.

Our results suggest a composite deformation related to magmatic deformation (preferred orientation and prismatic clinopyroxene) to impact event(s) (single grain internal deformation and twinning).

REFERENCES

Stolper E. M. McSween H. Y. and Hays J. F., 1979. Geochimica Cosmochimica Acta. A petrogenetic model of the relationships among achondritic meteorites. 43: 589-602.

McCoy T. J., Taylor G. J. and Keil K., 1992. Geochimica Cosmochimica Acta. Zagami: Product of a two-stage magmatic history. 56: 3571-3582.

1.4

The effect of melting and crustal production on plate tectonics on terrestrial planets

Lourenço Diogo L.[1], Tackley Paul J.[1]

[1] *Institute of Geophysics, ETH Zurich, Sonneggstrasse 5 (NO), CH-8092 Zurich, Switzerland (diogo.lourenco@erdw.ethz.ch)*

Within the Solar System, Earth is the only planet to be in a mobile-lid regime, whilst it is generally accepted that all the other terrestrial planets are currently in a stagnant-lid regime, showing little or no surface motion. A transitional regime between these two, showing episodic overturns of an unstable stagnant lid, is also possible and has been proposed for Venus.

Using plastic yielding to self-consistently generate plate tectonics on an Earth-like planet with strongly temperature-dependent viscosity is now well-established, but such models typically focus on purely thermal convection, whereas compositional variations in the lithosphere can alter the stress state and greatly influence the likelihood of plate tectonics. For example, Rolf and Tackley (2011) showed that the addition of a continent can reduce the critical yield stress for mobile-lid behaviour by a factor of around 2. Moreover, it has been shown that the final state of the system (stagnant- or mobile-lid) can depend on the initial condition (Tackley, 2000); Weller and Lenardic (2012) found that the parameter range in which two solutions are obtained increases with viscosity contrast.

We can also say that partial melting has a major role in the long-term evolution of rocky planets: (1) partial melting causes differentiation in both major elements (like Fe and Si) and trace elements, which are generally incompatible. Trace elements may contain heat-producing isotopes, which contribute to the heat loss from the interior; (2) melting and volcanism are an important heat loss mechanism at early times that act as a strong thermostat, buffering mantle temperatures and preventing it from getting too hot; (3) mantle melting dehydrates and hardens the shallow part of the mantle and introduces viscosity and compositional stratifications in the shallow mantle due to viscosity variations with the loss of hydrogen upon melting (Korenaga and Karato, 2008).

In this work we present a set of 2D spherical annulus simulations using StagYY (Tackley, 2008), which uses a finite-volume scheme for advection of temperature, a multigrid solver to obtain a velocity-pressure solution at each timestep, tracers to track composition, and a treatment of partial melting and crustal formation. We address the question whether melting-induced crustal production changes the critical yield stress needed to obtain mobile-lid behaviour as a function of governing parameters.

Our results show that melting and crustal production strongly influence plate tectonics on terrestrial planets, by making plate tectonics both easier and harder; i.e., for the same yield stress and reference viscosity the use or not of a treatment for melting and crustal production may result in a change from a stagnant-lid regime into an episodic-lid regime or a change from mobile-lid regime to an episodic-lid regime. Several factors can play a role on these, namely lateral heterogeneities and differences in the lid thickness induced by melting and crustal production, the maximum depth of melting, etc.

REFERENCES

Korenaga, J., & Karato, S. I. (2008): A new analysis of experimental data olivine rheology, Journal of Geophysical Research, 113(B02403).

Rolf, T., & Tackley, P. J. (2011): Focussing of stress by continents in 3D spherical mantle convection with self-consistent plate tectonics, Geophysical Research Letters, 38(18).

Tackley, P. J. (2000): Self-consistent generation of tectonic plates in time-dependent, three-dimensional mantle convection simulations, Geochemistry, Geophysics, Geosystems, 1(1).

Tackley, P. J. (2008): Modelling compressible mantle convection with large viscosity contrasts in a three-dimensional spherical shell using the yin-yang grid, Physics of the Earth and Planetary Interiors, 171(1-4), 7-18.

Weller, M. B., & Lenardic, A. (2012): Hysteresis in mantle convection: Plate tectonics systems, Geophysical Research Letters, 39(L10202).

1.5

The Baden-Irchel-Herdern Lineament: An inherited normal fault controlling the front of the eastern Jura fold-and-thrust belt

Malz Alexander[1], Madritsch Herfried[2], Meier Beat[3], Navabpour Payman[1], Heuberger Stefan[3/4] & Kley Jonas[5]

[1] *Institute of Geosciences, Friedrich-Schiller-University Jena, Burgweg 11, D-07749 Jena (alexander.malz@uni-jena.de)*
[2] *Nagra, Hardstraße 73, CH-5430 Wettingen*
[3] *Proseis AG Zürich, Schaffhauserstrasse 418, CH-8050 Zürich*
[4] *geosfer-ag, Büro für angewandte Geologie, Glockengasse 4. CH-9000 St.Gallen*
[5] *Georg-August-Universität Göttingen, Geowissenschaftliches Zentrum, Goldschmidtstr. 3, D-37077 Göttingen*

Thin-skinned fold-and-thrust belts around the world are described as the outer thrust front of orogens located in their forelands. In these areas a tectonically weak layer acts as the basal décollement over which the sedimentary overburden detaches and moves towards the foreland. In general these fold-and-thrust belts are considered to obey the kinematics of critical accretionary wedges, where the outer toe of the fold belt acts as the frontal thrust.

The Late Miocene to Early Pliocene Jura fold-and-thrust belt, stretching across northern Switzerland and eastern France, is an example of such a foreland fold-and-thrust belt, which consists of a series of mainly E–W trending folds and thrusts often referred to as Folded Jura. In our study area, comprising the easternmost part of the thrust belt, the border between the Folded Jura and the non-detached autochthonous foreland (Tabular Jura) is not clearly defined. In most interpretations, the frontal thrust is however defined by the northernmost anticline of the Folded Jura visible at the surface, which is in our case the prominent Lägern Anticline. Based on newly reprocessed, depth migrated seismic sections across the front of the Folded Jura, we analyse the Baden-Irchel-Herdern Lineament (BIH), a regional structure located north of the Lägern Anticline. The ENE-WSW trending fault zone coincides with the southern border fault of a deep Palaeozoic trough system. This trough was extensionally reactivated in Miocene times during the subsidence of the North Alpine Foreland Basin. Along the eastern part of the BIH, this reactivation is documented by normal offsets of the Tertiary Molasse sediments in seismic sections, as well as in outcrops. In our study area, the Baden-Irchel-Herdern Lineament indicates an additional contractional deformation overprint.

We used classical cross section balancing methods of equal line lengths and areas through an iterative research process of validation and reinterpretation to verify the geometry the BIH. Our results show that the best matching interpretation is to assume a complex triangle structure at the location where the basal décollement is ruptured by an inherited normal fault. The structure shows one major thrust in emerging from the main décollement horizon in Middle Triassic strata and a back-thrust rooting in Jurassic strata. According to this interpretation, the Uppermost Jurassic and Tertiary units form pop-up structure above the back-thrust. Next to this triangle structure, secondary high-angle thrusts and back-thrusts may indicate reverse reactivation of Tertiary normal faults during the contraction phase related with the formation of the Jura fold-and-thrust belt. Thereby, the BIH shows a very uniform amount of shortening over a relatively wide area. We interpret these equal shortening values as a kind of “structural saturation”, suggesting that the configuration of the structure has reached a maximum amount of deformation during an initial phase of Jura folding.

To the west of our study area the Baden-Irchel-Herdern Lineament merges with the frontal Jura thrust. At this location, the Lägern Anticline shows a conspicuous change in strike from an E-W to an ENE-WSW trend, the latter being parallel to the Baden-Irchel-Herdern Lineament. This strike change of the frontal thrust may imply that the BIH represents a kinematic “foreland stopper”, where the propagation of the thin-skinned frontal thrust ceased due to a disruption of the basal décollement along the inherited normal fault zone.

1.6

Rheology-driven phase equilibria and the in-situ formation of high-pressure rocks

Moulas Evangelos[1], Burg Jean-Pierre[1] & Podladchikov Yuri[2]

[1]*Department of Earth Sciences, ETH-Zurich, Sonneggstrasse 05, CH-8092 Zurich (evangelos.moulas@erdw.ethz.ch)*
[2]*Faculty of Geosciences and Environment, University of Lausanne, CH-1015 Lausanne, Switzerland*

Shear zones represent localised deformation in rocks, which directly depends on some weakening effect. Various processes such as viscous heating are responsible for decreasing the temperature-dependent viscosity in deforming shear zones that can be approximated as weak layers during deformation. Competent layers and boudins enhance the rheological heterogeneity where they are involved in the shear zones. Such heterogeneities cause perturbations in the pressure field if force balance is to be maintained.

The Kolosov-Muskhelishvili equations for elliptical bodies under slow viscous flow were employed to estimate the dynamic parameters (stress and pressure) and their relation to the far-field tectonic stress that generates deformation. Mohr-circle diagrams are used to illustrate the state-of-stress of deforming heterogeneities. The results show that pressure and stress perturbations depend strongly on the orientation of the far-field stresses with respect to the long axis of the elliptical heterogeneity. A viscosity ratio of 10 between the heterogeneity and the surrounding matrix is sufficient to produce pressure perturbations in with about the same magnitude as the far-field stress.

Comparison of the analytical solutions with thermo-mechanical models confirms such pressure perturbations and suggests that dynamic parameters such as pressure and temperature vary spatially and temporally in deforming zones. The dependence of metamorphic phase equilibrium on pressure and temperature implies that metamorphic rocks classified as high-pressure may form in-situ in collisional tectonic environments.

1.7

Probable Tsunami in the south Caspian Sea by a large earthquake!

Nazari Hamid[1], Ghorashi Manouchehr[1], Kaveh Firouz Ameneh[2]

[1] *Research Institute for Earth Sciences, Geological Survey of Iran, PO. Box: 13185-1494, Tehran- Iran. (h.nazari@gsi.ir)*
[2] *Geological Survey of Iran, PO. Box: 13185-1494, Tehran- Iran.*

The South Caspian basin is surrounded by the Central Alborz mountain range in south and Talesh Mountain in its south western side (Allen et al.,2003). The Central Alborz corresponds to the E-W trending and Talesh is corresponding to the NS trending that both of them bounding the Caspian Sea to the south and south west, as an active terrain belonging to the Alpine-Himalayan seismic belt (Jackson et al.,2002). The Khazar (Caspian) fault, nearly 450 kilometres long, and Astara fault, 110km long appear as the northern border of the Central Alborz and eastern border of the Talesh chain where Mesozoic and paleogene rock units overridden on the young deposits of the South Caspian plain(Nazari 2006). Base on Morphotectonics and Paleoseismology studies, we suggest that a major part of the present shortening in Alborz is localized on the Northern face of the chain along the Khazar fault zone; it is however worth noting that this contact might be located further to the North under the sea(Nazari 2006; Ritz et al., 2006). This border can be interpreted as frontal contact between Alborz and the South-Caspian basin. A recent stratigraphic study on the Holocene –Pleistocene in East of the Haraz valley, suggests an incision rate of 1.25 mm/yr as calculated for the last 12 Kyr. If it is assumed that the incision is related to the vertical component along the Khazar fault, the horizontal N-S shortening along this fault would be 2.5 mm/yr (for a 35° S-dipping fault). This is only 1/10th of the total shortening of Alborz, estimated 5 ± 2 mm/yr(Nazari 2006).

The Astara fault as major active fault system in south west of the SCB that regards to the seismic and geophysical observation propagated under the sea as well as the Khazar fault. Many earthquakes may have been caused by the activity of various branches of these fault systems in land or marine parts of the SCB.

regards to the basin geometry, propagated faults to north or east and its land slope, besides more than 20 km thickness of Neogene and Quaternary deposits in the south Caspian Basin in the scenario with the possibility of a seismic activity on the khazar or the Astara faults or one of the them propagated branches to the north and east with magnitude M ≥ 7, as the closest active faults to the great lake can trigger many large submarine earthquake ruptures or submarine landslides which is its potential for generating tsunamis in the steep southern coast. And if the tsunami wave height reaches to more than 5 meters, impact area could be estimated ~ 20 km especially in south east of the Caspian beach.

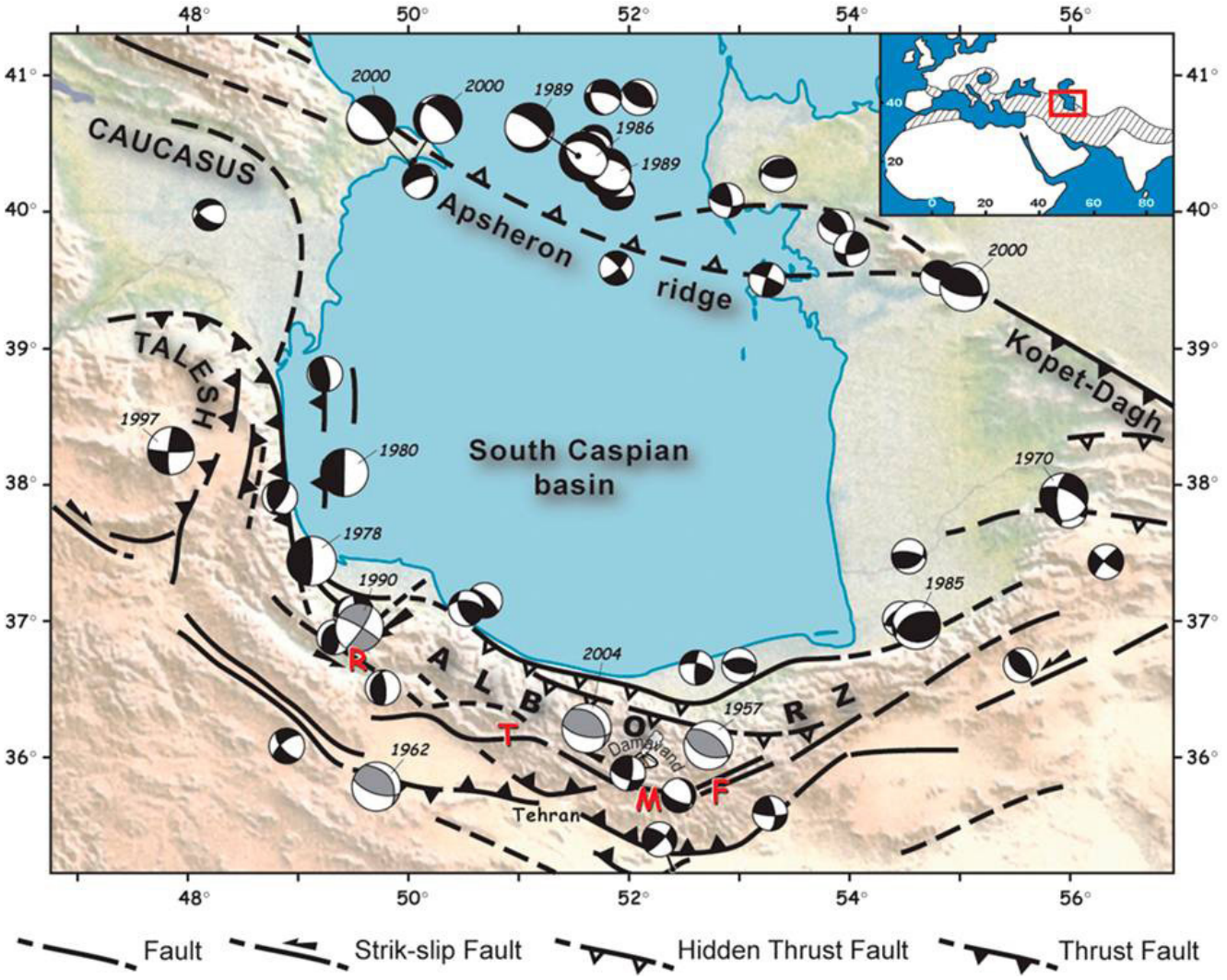

Figure 1. seismotectonic map of the South Caspian Basin(Ritz et al., 2006)

REFERENCES

Allen, M. B., Vincent, S.J.,Ian Alsop, G.,Ismail Zadeh, A. & Flecker, R. 2003. Late Cenozoic deformation in sout Caspian region : effects of a rigid basement block within a collision zone. Tectonophysics 366, 223-239.

Jackson, J., Priestley, K., Allen, M. & Berberian, M., 2002. Active tectonics of the South caspian Basin. Geophys. J. Int. 148, 214-245.

Nazari, H., 2006. Analyse de la tectonique recente et active dans l'Alborz Central et la region de Teheran:Approche morphotectonique et paleoseismologique. Science de la terre et de l'eau. Montpellier, Montpellier II: 247.

Ritz , J.-F., Nazari, H., Ghassemi,A., Salamati,R., Shafei, A., Solaymani,S.&Vernant, P., 2006. Active transtention inside Central Alborz: A new insight into the Northern Iran-Southern Caspian geodynamics, Geology, 34 (6), 477-480.

1.8

The internal structure of the Säntis nappe: folds, thrusts and wrench faults

Sala Paola[1], Pfiffner Adrian[1]

[1]*Institut für Geologie, University of Bern, Baltzerstrasse 1, CH-3012 Bern (sala@geo.unibe.ch)*

A 3D geological model (Sala et al. 2013) representative of an area of ca. 110 km2 was constructed on the base of a series of cross-sections (Schlatter 1941, Funk et al. 2000, Pfiffner 2011) to determine how shortening within the Säntis nappe varies along strike. The cross-sections were constructed and validated using the technique of line-length balancing.

Minimum shortening estimates vary from West to East, from 50% to 30%. This pattern is similar to the observed decreases in shortening in the confining Helvetic nappes in Western Austria (Zerlauth et al. 2013).

Retrodeformation of the Säntis nappe using the top of a mechanical strong unit (Schrattenkalk Formation) was performed to restore the nappe internal thrust faults and folds to their original position. An independent deformation history is recognized in the Western part of the model, where the amount of shortening is higher than the eastern block and where an internal partitioning shows an increase of 10% shortening in the frontal part of the nappe.

REFERENCES

Funk, H., Habicht, K. J., Hantke, R., & Pfiffner, O. 2000: Blatt 1115 Säntis. - Geol. Atlas Schweiz 1:25.000, erläut. 78. Bern: Bundesamt für Wasser und Geologie., pp. 61.

Pfiffner, A. 2011: Structural map of the Helvetic Zone of the Swiss Alps including Vorarlberg (Austria) and Haute Savoie (France). Geological Special Map 1:100.000, Explanatory notes., Federal Office of Topography Swisstopo.

Sala P., Pfiffner A., Frehner, M. 2013: The Alpstein in three dimensions: fold-and-thrust belt visualization in the Helvetic zone, Switzerland. Submitted to Swiss Journal of Geosciences.

Schlatter, L. 1941: Neue Geologische Untersuchungen in Mittleren Säntisgebirge. Ph.D. thesis, St. Gallen, Zollikofer & co.

Zerlauth, M., Ortner, H., Pomella, H., Pfiffner, A., & Fügenschuh, B. 2013: Inherited tectonic structures controlling the deformation style - an example from the Helvetic nappes between eastern Switzerland and Upper Allgäu (Bavaria). Swiss Journal of Geoscience, in press.

1.9

Kinematics and 3D pattern of ductile shear zones in the Gruebensee-Gelmersee transect (Hasli Valley, central Switzerland).

Schubert Raphael[1] and Herwegh Marco [1],

[1]*Geologisches Institutt, University of Berne, Baltzerstrasse 3, CH-3012 (raphael.schubert@students.unibe.ch)*

Within a master study, special emphasis has been paid to the evolution, the spatial distribution and the 3D geometry of ductile shear zones in the Central Aar granite (CAGr) and Mittagsfluh granite (MiGr) in the transect Grubensee – Gelmersee (Hasli valley, central Switzerland). For this purpose, the shear zone pattern was mapped in detail at the surface as well as in several underground facilities. Based on the surface information (map and orientation measurements) the planes of the shear zones were projected to depth and a 3D model was built with the Move™, a Midland Valley software. The interpolation of the surface data and the underground data shows that all shear zones are steeply dipping. The building of the shear zones was done according to the dip azimuth and the dip measured on the surface and of a best-fit plane. The quality of the surface-based projections to depth of the 3D-model was evaluated by the misfit between the constructed planes of shear zones and those actually found in tunnels. An average misfit of 3.75% was estimated.

Basically, two major shear zone sets can be discriminated. The first set is NE-SW striking and subparallel to magmatic anisotropies, like magmatic foliations. It is characterized by steep south dipping lineations showing normal and reverse faulting. The second set is NW-SE striking and shows subhorizontal lineations representing strike slip faulting. Crosscutting relationships indicate that the NW-SE set is younger than the NE-SW one. While the first set is interpreted to reflect early thrust related shearing, the second set probably evolved due to transpression of an over-thickened continental crust. In this way, the max prinicipal stress axis ($\sigma1$) remained constant over time, but $\sigma2$ and $\sigma3$ flipped. Consequently, ongoing compression induced lateral escape of material leading to the formation of the strike-slip shear zones. As a special feature, the NW-SE shear zones are turning into an E-W direction in the northern part of the working area, where the MiGr is located. This can be explained by ongoing compression, where the MiGr acted as a mechanically rigid body. In this way, inherited magmatic anisotropies control the style and evolution of the early Alpine shear zones, which are then brittly reactivated during a younger stage.

1.10

Orographic precipitations need glaciers to control long-term erosion rates and topography of tectonically inactive mountain ranges

Thibaud Simon-Labric[1], Peter W. Reiners[2], Jean Braun[3]

[1] *Institut des Sciences de la Terre (ISTE), Université de Lausanne (UNIL), 1015 Lausanne, Suisse.*
[2]. *Geosciences, University of Arizona, Tucson, AZ, USA.*
[3] *Institut des Sciences de la Terre (Isterre), Université Joseph Fourier, BP53, 38041 Grenoble, France.*

It is well known that mountain topography gives rise to some of the most pronounced climate gradients on Earth, the orographic precipitation, but his role on erosion pattern and interactions between the atmosphere and the rest of the Earth System remains poorly understood. The Washington Cascades is a mountain belt particularly sensitive to climate and offers correlations among modern orographic precipitation and erosion rates from 104 to 107 years. Here we use an extensive apatite (U-Th)/He thermochronology data set and thermal-kinematic modeling to reconstruct the erosional and topographic evolution of the range since 15 Myr and show that the forcing of the erosion pattern of the range by orographic precipitation do not start with the onset of orographic precipitation in the Middle-Late Miocene but around the time of the Plio-Quaternary transition. We find a five-time increase of the erosion on the humid side of the range producing a 10 km retreat of the main drainage divide in direction of the arid flank and conclude that the shift from fluvial to glacial-interglacial processes had been necessary to couple precipitation and erosion patterns.

1.11

Structural and morphoplogical changes in the shallow plate boundary system and trench, triggered by rare subduction megathrust earthquakes

Strasser Michael[1], Kodaira Shuichi[2] Dinten Dominik[1],

[1]*Geological Institute, ETH Zurich, Sonneggstrasse 5, CH-8092 Zurich (strasser@erdw.ethz.ch)*
[2]*Japan Agency of Marine-Earth Science and Technology (JAMSTEC), 2-15 Natsushima-Cho, Yokosuka-city, Kanagawa 237-0061, Japan*

Topography and structures of frontal prisms in shallow plate boundary systems along subduction margins generally are assumed to reflect compressional tectonics in marine sediments. In contrast, also gravitational instability, prism collapses or submarine slumps can affect the shallow convergent plate boundary system, and often are hypothesized to be triggered by earthquakes. This study aims at (i) investigating this interplay between overall compressional vs. sporadic gravitational tectonics and subduction megathrust earthquakes; and at (ii) exploring rates and frequencies of processes and events governing the structural and morphological evolution of the frontal prism and trench system. The focus is on the Japan Trench subduction zone that ruptured in 2011 in the magnitude 9 Tohoku-oki earthquake off Japan.

We present bathymetric and reflection seismic data obtained before and after the 2011 earthquake, along with sediment cores, retrieved in 2012 from the >7km deep Japan Trench. Our data document significant seafloor- and subseafloor changes as tectonic and geomorphic expressions of this mega-earthquake. In particular, we present several lines of evidence for a large (> 27.7 km2) slump in the trench and interpret a causal link between earthquake slip to the trench and rotational slumping above a subducting horst structure, which significantly impacted the geometry and evolution of the shallow plate boundary system by emerging a new submarine fold-and-thrust. This implies that earthquake-triggered slumps can be leading agents for accretion of trench sediments into the forearc and that forward growth of the prism and seaward advance of the deformation front by several kilometres can occur, punctuated, during a single-event large mega-thrust earthquake.

We further use numerical frontal prism stability models which include transient stresses due to seismic ground motion and scenarios for a complete stress drop along the décollement to constrain our conceptual interpretation based on the seafloor and sub-seafloor data and samples. Model results reproduce deep-seated rotational gravitational instability in the frontal prism, but also indicated that slip-to-the trench and >M.8.5 earthquakes are needed to trigger the observed instability and deformation. This suggests that only rare mega-events, such as the 2011 Tohoku-oki earthquake, which may have recurrence patterns in the order of 1000 years, can impart sudden structural and morphoplogical changes in the shallow plate boundary system and trench.

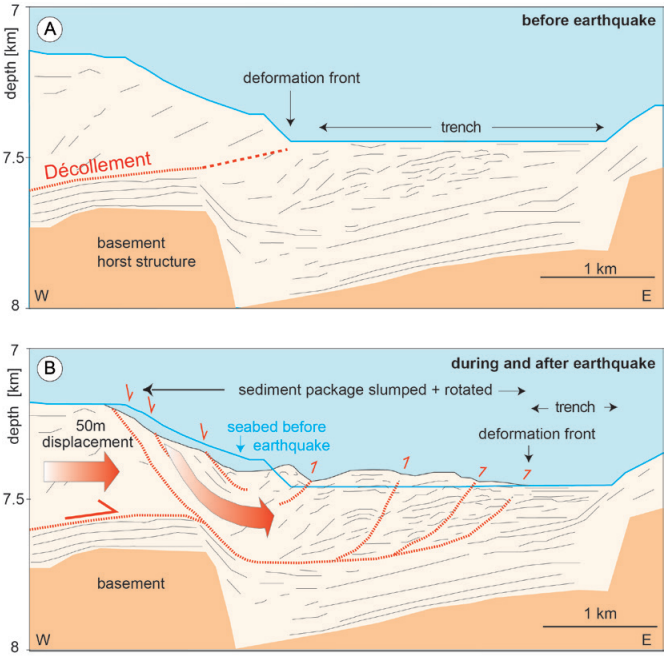

Figure 1. Conceptual sketch modified after Strasser et al., 2013 proposing a causal link between (1) earthquake rupture to the trench, (2) rotational slumping induced by co-seismic displacement of the sedimentary block above the horst structure over the graben, and (3) compressional effects resulting in forward imbrication and accretion of trench material into a 2–3-km-wide emerging submarine fold-and-thrust belt. Deformation front advances seaward by 2–3 km, establishing a new frontal thrust/décollement system in Japan Trench after the earthquake.

REFERENCES

Strasser M., et al., 2013: A Slump in the Trench: Tracking the impact of the 2011 Tohoku-Oki earthquake, Geology, 41, 935-938.

1.12

Exhumation history, topographic relief evolution and geothermal activity in the Swiss Central Alps (Rhône valley): insights from low-temperature thermochronology

Pierre G. Valla[1,2], Meinert Rahn[3,4], David L. Shuster[5,6] & Peter A. van der Beek[7]

[1.] *Geological Institute, ETH Zürich, Sonneggstrasse 5, CH-8092 Zürich (pierre.valla@erdw.ethz.ch)*
[2.] *Institute of Earth Sciences, University of Lausanne, Géopolis, CH-1015 Lausanne*
[3.] *Swiss Federal Nuclear Safety Inspectorate, Industriestrasse 19, CH-5200 Brugg*
[4.] *Department of Mineralogy and Geochemistry, Albert-Ludwigs-Universität, Albertstrasse 23b, D-79104 Freiburg*
[5.] *Department of Earth & Planetary Science, University of California, 479 McCone Hall, USA-94720 Berkeley*
[6.] *Berkeley Geochronology Center, 2455 Ridge Road, USA-94707 Berkeley*
[7.] *Institute of Earth Sciences, University of Grenoble, 1381 Rue de la Piscine, F-38041 Grenoble*

The Neogene evolution of the European Alps and potential climatic and/or tectonic controls on denudation rates and relief development during the late-stage exhumation remain subjects of scientific debate (e.g. Willett, 2010). Late Cenozoic to Plio-Quaternary increases in both *in-situ* denudation rates and sediment flux to surrounding basins are suggested to have been caused by climatically-induced relief amplification (Kuhlemann et al., 2002; Vernon et al., 2008). However, even though geomorphologic and sedimentologic studies both suggest topographic relief change and transition from fluvial to oscillations between glacial/fluvial conditions (Muttoni et al., 2003; Norton et al., 2011), precise quantifications on both the timing and magnitude of this transition are only sparse (Häuselmann et al., 2007).

In this study, we focus on the upper Rhône valley (Swiss Central Alps) within the Visp-Brig area (Aar massif, Valais). This area shows among the highest late Neogene exhumation rates within the Western-Central European Alps (Vernon et al., 2008), influenced by tectonic activity along the major Simplon-Rhône extensional fault system (e.g. Mancktelow, 1985, Campani et al., 2010). Moreover, the upper Rhône valley has experienced enhanced glacial erosion associated with strong relief development during the Pliocene-Quaternary period (Norton et al., 2011; Valla et al., 2011). Finally, structural inheritance, late-stage tectonics and rapid exhumation may have promoted recent hydrothermal activity in this region (Sonney and Vuataz, 2008).

We have addressed these aspects and their potential interaction on the cooling history by using different low-temperature thermochronometers along a pseudo-vertical bedrock profile with additional samples from a geothermal well (Brigerbad). Bedrock samples come from elevations between 600 and 2900 m and were combined with samples from a 500-m depth drilling well, resulting in a total ~3 km elevation difference. Apatite fission-track (AFT) dating, as well as track-length data, have been added to previously published (Valla et al., 2011) and new apatite (U-Th-Sm)/He (AHe) and $^{4}He/^{3}He$ data.

Our AFT and AHe results reveal high-exhumation rates (~1 km/Myr) within late-Cenozoic to Pliocene times, while $^{4}He/^{3}He$ data confirm this exhumation pulse (Valla et al., 2011). $^{4}He/^{3}He$ data from valley bottom samples, confirmed by AHe data from the drilling well, show a rapid increase in late-stage exhumation associated to the onset of major Alpine glaciation triggering valley carving. Apatite track length measurements suggest that well samples have been affected by recent hydrothermal activity.

REFERENCES

Campani, M., Herman, F. & Mancktelow, N. 2010. Two- and threedimensional thermal modeling of a low-angle detachment: Exhumation history of the Simplon Fault Zone, central Alps. Journal of Geophysical Research, 115, B10420.

Häuselmann, P., Granger, D.E., Jeannin, P.-Y. & Lauritzen, S.-E. 2007. Abrupt glacial valley incision at 0.8 Ma dated from cave deposits in Switzerland.
Geology, 35, 143-146.

Kuhlemann, J., Frisch, W., Szekely, B., Dunkl, I. & Kazmer, M. 2002. Post-collisional sediment budget history of the Alps: Tectonic versus climatic Control. International Journal of Earth Sciences, 91, 818-837.

Mancktelow, N. 1985. The Simplon Line: A major displacement zone in the Western Lepontine Alps. Eclogae Geologicae Helveticae, 78, 73-96.

Muttoni, G., Carcano, C., Garzanti, E., Ghielmi, M., Piccin, A., Pini, R., Rogledi, S. & Sciunnach, D. 2003. Onset of major Pleistocene glaciations in the Alps. Geology, 31, 989-992.

Norton, K.P., Abbühl, L.M. & Schlunegger, F. 2010. Glacial conditioning as an erosional driving force in the central Alps. Geology, 38, 655-658.

Sonney, R. & Vuattaz, F.-D. 2008. Properties of geothermal fluids in Switzerland: A new interactive database. Geothermics, 37, 496-509.
Valla, P. G., Shuster, D.L. & van der Beek, P.A. 2011. Major increase in relief of the European Alps during mid-Pleistocene glaciations recorded by apatite 4He/3He thermochronometry. Nature Geoscience, 4, 688-692.
Vernon, A.J., van der Beek, P.A., Sinclair, H.D. & Rahn, M.K. 2008. Increase in late Neogene denudation of the European Alps confirmed by analysis of a fission track thermochronology database. Earth and Planetary Science Letters, 270, 316-329.
Willett, S.D. 2010. Late Neogene Erosion of the Alps: A Climate Driver? Annual Review of Earth and Planetary Sciences, 38, 411-437.

1.13

Fluid involved, high grade cataclasis during Alpine ductile deformation in basement rocks of the Aar massif

Wehrens Philip[1], Herwegh Marco[1], Berger Alfons[1]

[1]*Institute of Geological Sciences, University of Bern, Baltzerstrasse 1+3, 3012 Bern (philip.wehrens@geo.unibe.ch)*

The Aar massif belongs to the external massifs of the Alps and is mainly composed of granitoids and gneisses. Post-Variscan granitoid rocks have intruded old gneisses (Altkristallin) belonging to the pre-Variscan basement. Despite numerous detailed studies in the past decades, the overall exhumation history and the associated massif internal deformation (internal strain distribution and its evolution in time) is largely unknown at present. Here we aim to provide insides into the relation between strain, fluid, rheology and their role in shear zone initiation, progression and localization.

Shear zone initiation and evolution is studied at a variety of scales along shear zones located at the southern margin of the Aar massif (from Rätrichsbodensee to Grimselpasshöhe). Detailed field mapping combined with microscopic analysis along strain gradients has been carried out.

During the Alpine orogeny, strain localized and re-activated along the following pre-existing mechanical anisotropies: i) Lithological variations between Post-Variscan intrusives and Pre-Variscan basement as well as between primary magmatic features (i.e., varying mica content in the Post-Variscan intrusive), ii) pre-existing Pre-Variscan and Variscan brittle and ductile faults.

During the Alpine orogeny alternations of ductile and brittle deformation have affected the host rocks. In domains weakly affected by Alpine deformation, dynamically recrystallized quartz grains indicate ductile deformation by subgrain rotation followed by a static overprint. Despite this ductile background strain, several microstructures indicate a coeval activity of hydrofracking. (i) Overprinting of the aforementioned ductile structures, by fractures along which biotite and epidote have precipitated and (ii) ultracataclasites overgrown by biotite. The fact that both fracture infill and mineral overgrowths consist of biotite suggest formation temperatures above 400°C, i.e. metamorphic conditions under which quartz deforms in a ductile manner. The only explanation for the simultaneous occurrence of brittle and ductile deformation structures at these elevated temperatures is a fast strain rate, which typically occurs during seismic events. We therefore postulate that our structures document seismic cycles characterized by fast brittle deformation followed by subsequent aseismic periods of ductile creep.

White mica and chlorite overgrowth of biotite on the previously described ductile shear zones indicate continuous shearing during retrograde metamorphic cooling. The retrograde decay of feldspars in form of fine-grained reaction products combined with a decrease in crystal plastic deformation of quartz, forced deformation to localize in these ultrafine-grained and thin high strain zones. With ongoing uplift and exhumation these late ductile shear zones are replaced by different generations of cataclasites which cut and/or reactivate the aforementioned precursor structures during the subsequent late stage deformation.

Altogether, this sequence shows the complex history of strain localization and the involvement of both brittle and ductile processes under the presence of fluids at elevated temperatures (>400°C). These conditions fit excellently with the base of the recent seismogenic zone underneath the Aar massif. We therefore suggest that the structural relations nowadays exposed in the Grimsel area give insights on the origin of today's earthquake activity at depths of about 12-15km.

P 1.1

On the origin of the Naybandan Arc-shaped structures, Tabas, Central Iran

Bagheri Sasan[1] & Sarani Maryam[1]

[1]*Department of geology, University of Sistan and Baluchestan, 98135 Zahedan, Iran*

The Tabas Block, a lens shaped continental tectonic sliver, which is surrounded by the Lut and Yazd Blocks in central Iran, and bordered by the two fault systems of Nayband and Kalmard-Kuhbanan, is the host of at least three arc-shaped structures which extend through the width of the block along the lens's short diameter. The presence of such EW-trending structures among the NS-trending ones is the main theme of this research. Each arc has a NE curvature at its eastern termination where it is separated from the Nayband fault, but gradually changes to an EW smooth trend at the middle and abruptly breaks into a NS trend where it joins the Western Tabas fold belt. The northeastern sloping part of each arc is characterized by south-westward-dipping thrusts which brought up the deeper rock of the crust onto the younger sedimentary rocks. Inside of each arc, structures similar to the dome and basin interference fold pattern can be observed, which may have occurred either as a result of two separate deformational events or during a long progressive deformation; the pattern which cannot be addressed outside of the arcs. Because the youngest sediment, such as the Paleocene Kerman Conglomerate south of the Tabas Block, has been affected by the aforementioned deformations, whereas the Oligocene pyroclastic rock covers the arc-shape structures with a pronounced angular nonconformity, the age of arc formation must be late Paleogene.

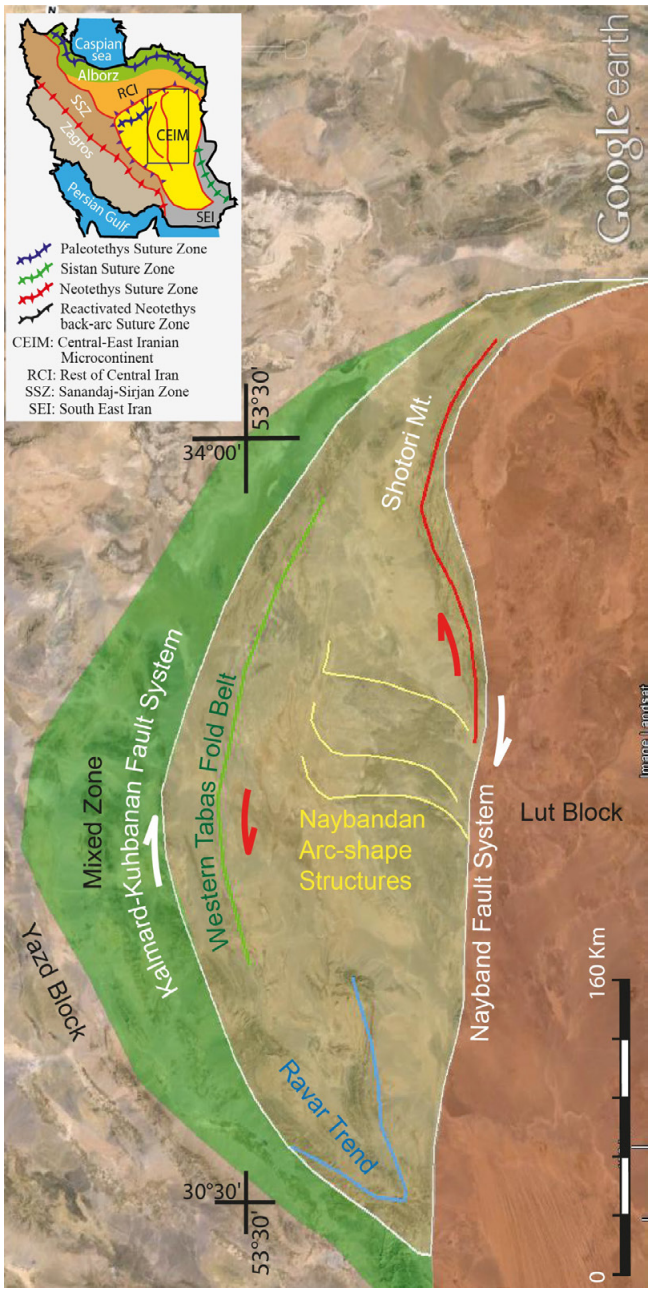

On a large-scale view, the Naybandan arc-shaped structures can be viewed as a portion of the large Tabas sigmoidal structure which closely follows the style of the Shotori Mountains (Figure 1), but with a difference of about 90° when we rotate anticlockwisely the sigmoidal around a vertical axis. We propose that the Tabas sigmoidal is a large deflection which appeared during the anticlockwise rotation of the Lut block. The essential role of the right-lateral strike-slip faults around the Tabas Block during the Paleogene period cannot be denied. The interference fold pattern mentioned above can be interpreted as the structures which originated during the distortion of the first set of folds formed at the primary stage of block rotation. Subsequently, the appearance of the NE-trending, right-lateral, strike-slip faults which dissected this sigmoid probably has been developed in continuation of the deflection. These faults are different from the NE-trending left-lateral strike-slip faults which have been activated since the Neogene time by another mechanism, such as the Doruneh fault.

Figure 1: Location of the Tabas Block in the simplified tectonic map of central Iran

P 1.2

2D thermo-mechanical modeling of basement-cover deformation with application to the Western Alps

Arthur Bauville[1] & Stefan M. Schmalholz[1]

[1]*ISTE, University of Lausanne, CH-1015 Lausanne (Arthur.bauville@unil.ch)*

The external crystalline massifs of Western Alps and the Helvetic sedimentary nappe stack result from the deformation of the European passive margin during the Alpine collision. This area has been studied extensively for the past hundred years. However although the geometry and tectonic structures are well documented, the mechanical behavior of the rocks during nappe stacking and basin inversion is still highly debated. The aim of this study is to reproduce the first order tectonic structures of the Western external Alps. We use a 2-D thermo-mechanical finite element model with visco-elasto-plastic rheology formulation to simulate the deformation of half-graben structures during collision. We systematically investigate the control of (1) the rheology, i.e. ductile vs brittle; linear vs power-law viscous rheology, and (2) the boundary condition, i.e. pure shear vs simple shear. Geometry and finite deformation patterns in both basement and sediments are then compared to cross-sections, finite strain ellipses and cleavage orientation from published field data. Orientation and distribution of plastic shear bands in the model are compared to fault distribution from field data and sand box analogue models.

P 1.3

Tectonosedimentary evolution of the Nankai forearc (Japan) constrained by detrital minerals in off-shore (IODP) drill sites and modern river beds

Buchs David[1], Cukur Deniz[2], Masago Hideki[3]

[1] *School of Earth and Ocean Sciences, Cardiff University, Main Building, Cardiff CF10 3AT, UK (buchsd@cf.ac.uk)*
[2] *GEOMAR Helmholtz Centre for Ocean Research Kiel, Wischhofstraße 1-3, D-24148 Kiel*
[3] *CDEX-JAMSTEC, 3173-25 Kanazawa-ku, Yokohama, 2360001, Japan*

The evolution of the Nankai forearc (central and SW Japan, Fig. 1) since the Pliocene has been primarily controlled by subduction of the Philippine Sea Plate under the Eurasian Plate, collision of the Izu-Bonin volcanic arc with Japan, and construction of a large accretionary prism by successive sediment stacking. Characterising the evolution of the forearc is central to the Nankai Trough Seismogenic Zone Experiment (NanTroSEIZE) of the Integrated Ocean Drilling Program (IODP), which aims at improving our understanding of processes ultimately leading to the formation of large earthquakes.

Seismic profiles and drilling in the framework of the NanTroSEIZE have shown that the forearc in SW Japan (Kumano transect, Fig. 1) includes contrasted structural domains, with, from NW to SE, a forearc basin, a megasplay fault zone, and imbricate and frontal thrust zones (Moore et al. 2009; Fig. 2).

Sedimentary and tectonic processes in the forearc together with the supply of detrital material to the Nankai Trough have played an important role in the recent evolution of the margin (Underwood and Moore 2013). Our study investigates the tectonosedimentary evolution of the upper forearc slope and Kumano forearc basin since the Pliocene using a sediment provenance analysis with samples collected in 8 major Japanese rivers and 3 drill sites (Figs 1 and 2). Our results show that cuttings samples, collected for the first time by the IODP during the NanTroSEIZE, can be successfully used to characterise the composition of sediments recovered by destructive drilling mode (i.e., without core recovery). In addition, the composition of detrital pyroxenes and amphiboles from our samples allow to identify the main sources of turbiditic deposits in the upper forearc, and provide new constraints on sedimentary patterns prior and during the development of the Kumano Basin. Integration of these data with a regional seismic profile along the Kumano transect provides new insights into the mode and timing of development of the Kumano Basin and its relationship with the development of the megasplay fault in underlying accretionary complex. A reconstruction of the evolution of the upper slope and Kumano Basin enlightens tectonosedimentary processes at tectonically-active subduction zones and provides a model for similar areas elsewhere.

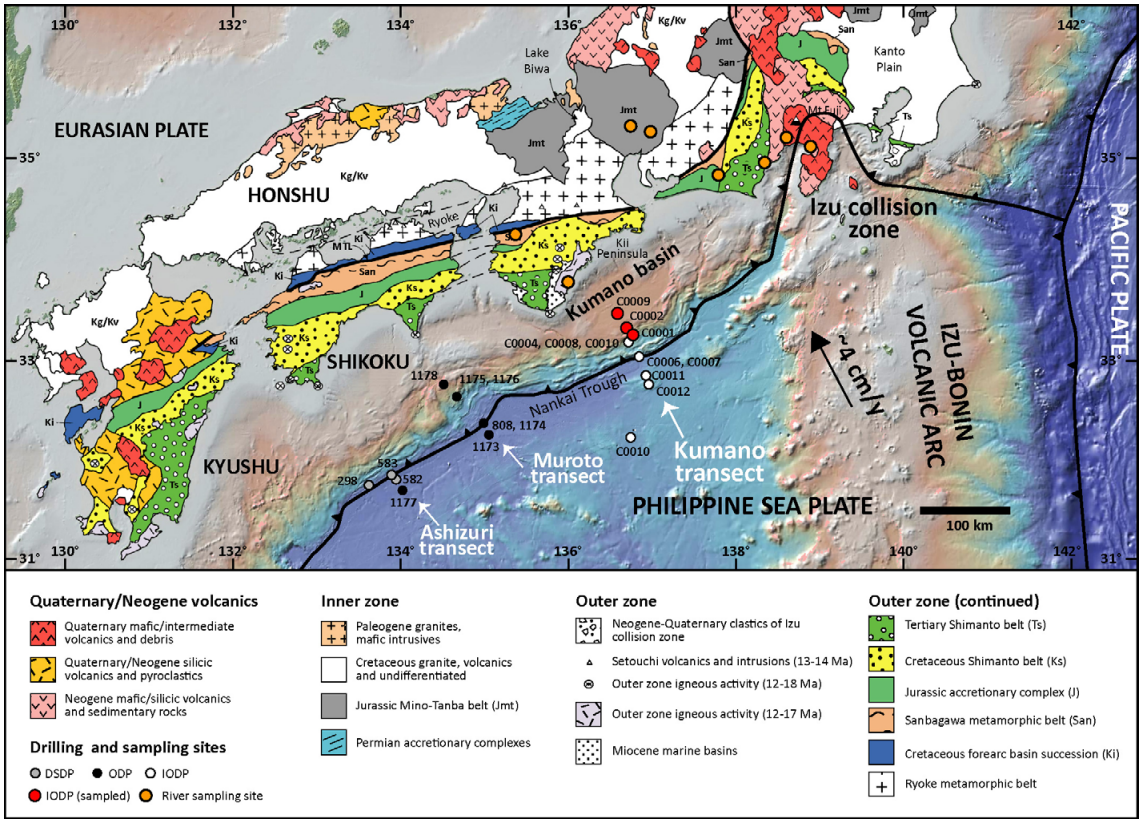

Figure 1. Simplified geological map of SW and central Japan (modified after Fergusson 2003), with location of off-shore (IODP) and on-land (river beds) samples used in this study.

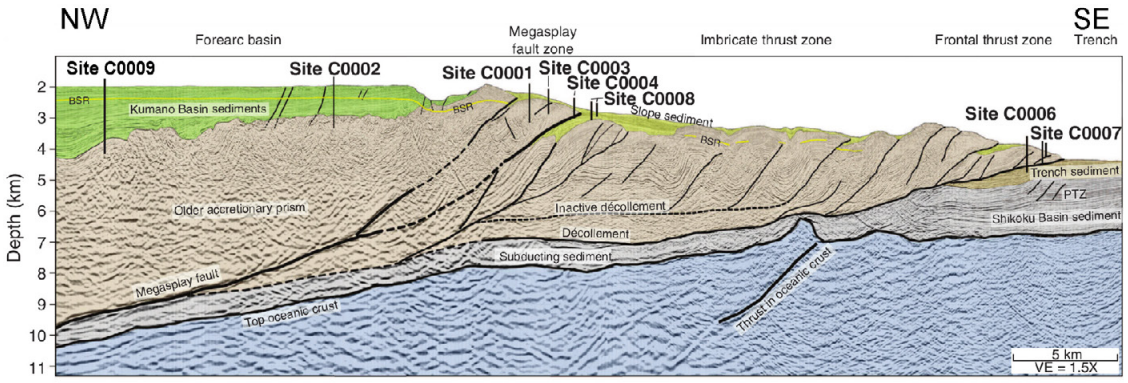

Figure 2. Main structures of the forearc along the Kumano transect (after Moore et al. 2009). Drill sites used in this study include C0001, C0002 and C0009 in the upper forearc slope and Kumano Basin.

REFERENCES

Fergusson, C.L., 2003. Provenance of Miocene–Pleistocene turbidite sands and sandstones, Nankai Trough, Ocean Drilling Program Leg 190. In Mikada, H., Moore, G.F., Taira, A., Becker, K., Moore, J.C., and Klaus, A. (Eds.), Proceedings of the ODP, Scientific Results, 190/196, 1–28.

Moore, G.F., Park, J.-O., Bangs, N.L., Gulick, S.P., Tobin, H.J., Nakamura, Y., Sato, S., Tsuji, T., Yoro, T., Tanaka, H., Uraki, S., Kido, Y., Sanada, Y., Kuramoto, S., and Taira, A., 2009. Structural and seismic stratigraphic framework of the NanTroSEIZE Stage 1 transect. In Kinoshita, M., Tobin, H., Ashi, J., Kimura, G., Lallement, S., Screaton, E.J., Curewitz, D., Masago, H., Moe, K.T., and the Expedition 314/315/316 Scientists, Proceedings of the IODP, 314/315/316, 1–46.

Underwood, M.B., Moore, G.F., 2012. Evolution of Sedimentary Environments in the Subduction Zone v of Southwest Japan: Recent Results from the NanTroSEIZE Kumano Transect, in: Busby, C., Azor, A. (Eds.), Tectonics of Sedimentary Basins: Recent Advances. John Wiley & Sons, Ltd, 310–328.

P 1.4

Geospeedometry of inverted metamorphic gradients of a crustal-scale thrust zone: first approach

Cioldi Stefania, Moulas Evangelos & Burg Jean-Pierre

Geological Institute, ETH Zurich, Sonneggstrasse 5, CH-8092 Zurich
(stefania.cioldi@erdw.ethz.ch, evangelos.moulas@erdw.ethz.ch, jean-pierre.burg@erdw.ethz.ch)

Thrust tectonics and inverted metamorphic gradients are major consequences of large and likely fast movements in compressional environments. These zones reportedly preserve high-grade metamorphic rocks in the hanging wall and inverted isograds in the footwall of the major thrust zone and occur in tectonic settings ranging from continent-continent collision to subduction zones.

The purpose of this study is to investigate the tectonic setting and the timescale of inverted metamorphic zonation due to crustal-scale thrusting. The aim is to contribute to understand the link between mechanical and thermal evolution of major thrust zones and to clarify the nature and the origin of orogenic heat. Chemical zoning profiles in garnet combined with mineral chemistry from the other minerals in the assemblage are useful indicators of pressure and temperature history of metamorphic rocks. In order to constrain the duration of the thermal event, 40Ar/39Ar geochronology offers a temporal resolution with the potential to characterized shear zone movement.

The first case-study is the Nestos thrust in the Rhodope metamorphic complex (Greece). The Rhodope massif is interpreted to be a deformed segment of the Alpine-Himalaya suture and represents a collisional system with an association of structures of both large-scale thrusting and pervasive exhumation tectonics. The study area is divided into three sections across the Nestos Shear Zone (NSZ): Drama, Xanthi and Komotini regions. The inverted metamorphic zonation starts from chlorite-muscovite grade and reaches locally the kyanite-sillimanite grades with migmatites in the highest tectonic levels. The high temperature metamorphic overprint replaces the relics of an earlier high-pressure metamorphic event and constrains the anatexis to have occurred at crustal levels. An overview of the geology and the methods used in this project are presented.

P 1.5

Effects of surface processes on multilayer detachment folding: a numerical approach.

Collignon Marine [1], May Dave A.[2], Kaus Boris J.P. [3], and Fernandez Naiara [3]

[1] *Geological Institute ETH Zurich, Sonneggstrasse 5, 8092 Zurich, (marine.collignon@erdw.ethz.ch)*
[2] *Institute of Geophysics, ETH Zurich, Switzerland.*
[3] *Institut für Geowissenschaften, Johannes Gutenberg-Universität, Mainz, Germany.*

Over the past decades, the interaction between surface processes and development of mountain belts has been extensively studied. While syntectonic sedimentation appears to control the external development of the fold-and-thrust belts, erosion strongly influences the evolution of internal regions within mountain belts.

The effects of surface processes on brittle deformation have been thoroughly studied using analogue and numerical models of accretionary wedges, however, most of the numerical studies used a 2D model of deformation and/or a simple formulation for the surface processes, where both sedimentation and erosion are rarely present together. Coupled analogue models of deformation and surface processes are challenging, due to material and scaling issues, and often only reproduce two end-member cases (no erosion vs very strong erosion, where all the material is removed), but fail to investigate the transitional cases.

In contrast, interactions between surface processes and ductile deformation (e.g. multilayer detachment folding) have been poorly investigated.

Thin-skinned fold and thrust belts are seen as the result of compressional deformation of a sediment pile over a weak layer acting as a décollement level. The resulting surface expression has often been interpreted, based on geometrical criteria in terms of fault bend folds, propagation folds and/or detachment folds. A few analogue studies have demonstrated that fold morphology can be influenced by erosion rates or preferential localization of sedimentation, and additionally, that the fold growth can be stopped by increasing the supply of sediments.

Here we aim to numerically investigate the effects of surface processes and multilayer folding in three dimensions. For this purpose, we have developed a finite-element based landscape evolution model (both erosion and sedimentation) using PETSc, and coupled it to the 3D mechanical code LaMEM. The landscape evolution model uses a non-linear diffusion formulation (Simpson and Schlunegger, 2003), taking into account both hillslope and channel processes. We present here preliminary results of the coupling between sediment loading and folding.

P 1.6

Thermo-mechanical feedback and modelling of crustal-scale shear zones.

Thibault Duretz[1], Stefan M. Schmalholz[1]

[1] *Institut des Sciences de la Terre, University of Lausanne, UNIL Geopolis, CH-1015 Lausanne (thibault.duretz@unil.ch)*

The collision between continental plates results in the development of orogenic belts. It is well known that the development of crustal-scale shear zone is a common feature of orogenic structures. Ductile shear zones may develop at various structural levels and can be characterised by their metamorphic grade, which is quantified by petrological analysis. Ductile shear zones are often invoked as mechanism for the exhumation of high-pressure (HP) rocks, however their role in the formation of HP units is often debated.

State of the art geodynamic modelling of continental collision is usually used to model the genesis and exhumation of HP rocks. Nevertheless, it is a common approach to model continental collision by predefining shear zones and/or by employing constitutive models that introduce mesh dependency (e.g. strain softening). Mesh size dependency leads to difficult comparison between physical models and natural data since pressure and temperature cannot be accurately computed within modelled shear zones.

In this study, we employ thermo-mechanical modelling to model the self –consistent development of crustal-scale shear zones. Our approach allows for full coupling between momentum and energy equations by including viscous dissipation. We show that this methodology allows for the spontaneous development of shear zones around a cylindrical weak inclusion. Systematic numerical simulations are performed and the results suggest that shear zone dimensions are independent on the mesh resolution. Moreover, we demonstrate that these results can be achieved by using two different numerical methods, which are both popular methods in the geodynamic modelling community (Lagrangian finite elements and Eulerian-Lagrangian finite differences). These results show that thermo-mechanical feedback allows for the development of finite-width shear zones. Such models can therefore be reliably used to quantify stresses, pressure and strain rates in shear zones, and for the modelling of continental collision. Further developments will include comparison with natural data, with a particular focus on the Alpine orogeny.

P 1.7

Was plate tectonics different in a hotter Earth? History and evolution of subduction in the Precambrium

Fischer Ria[1], Gerya Taras[1]

[1] *Institute of Geophysics, ETH Zürich, Sonneggstrasse 5, CH-8092 Zürich (ria.fischer@erdw.ethz.ch)*

Plate tectonics is a global self-organising process driven by negative buoyancy at thermal boundary layers. Phanerozoic plate tectonics with its typical subduction and orogeny is relatively well understood and can be traced back in the geological records of the continents. Interpretations of geological, petrological and geochemical observations from Proterozoic and Archean orogenic belts however (e.g., Brown, 2006; Taylor and McLennan, 1995), suggest a different tectonic regime in the Precambrian. The lithosphere shows very low internal strength and is strongly weakened by percolating melts and increased temperature due to higher radioactive heating rates and secular cooling. The fundamental difference between Precambrian and Phanerozoic subduction is therefore the upper-mantle temperature, which determines the strength of the upper mantle and hence further subduction history.

3D petrological-thermomechanical numerical modelling experiments of oceanic subduction at an active plate margin done with the finite difference multigrid solver I3ELVIS (Gerya and Yuen, 2007) at increased upper-mantle temperature have been performed to model subduction under Precambrian conditions. Results show (1) an increased importance of small-scale convection with plume shaped cold downwellings replacing the large-scale cold downwelling at temperatures of +150 K to +200 K above present day upper mantle temperature. (2) Thickening of oceanic plates and thinning of continental plates leads to a tectonic style which does not distinct between oceanic and continental plates anymore but merely between two types of terrains, mafic and felsic, of the same thickness. (3) Fracture zones are rendered ineffective at high temperatures which, together with the thickening of oceanic crust, chokes the subduction zone and does not allow any subduction for temperatures above +200 K.

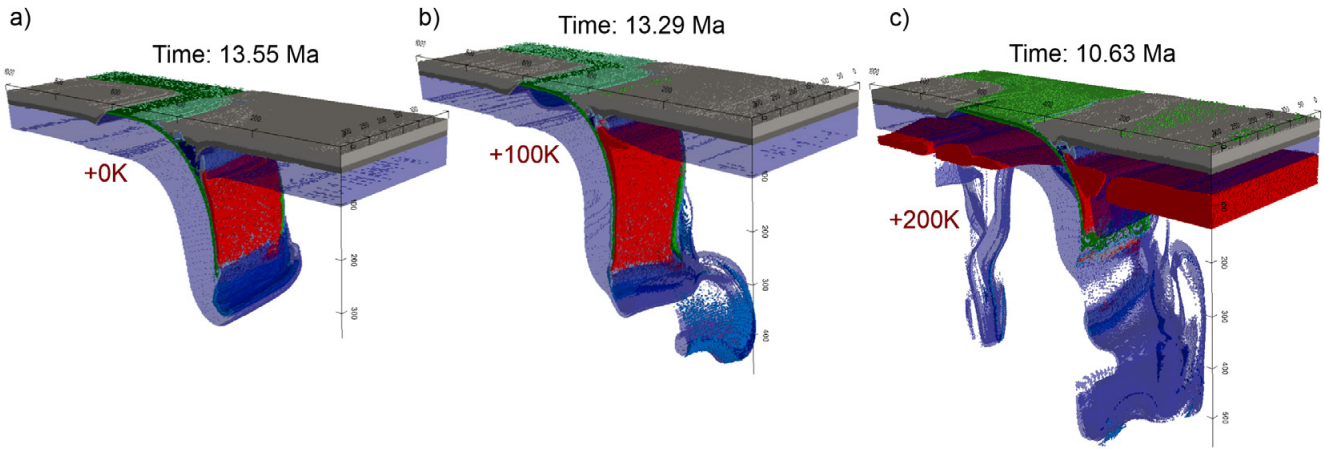

Figure 1. Subduction style depends strongly on upper mantle temperature. (a) Modern subduction with present day temperature gradients in upper-mantle and lithosphere. (b) Increase of temperature by 100 K at the lithosphere-asthenosphere boundary (LAB) leads to melting and drip-off of the of the slab-tip. (c) A temperature increase of 200 K leads Rayleigh-Taylor instabilities and delamination of the whole lithosphere.

REFERENCES:

Brown, M., 2006. Duality of thermal regimes is the distinctive characteristic of plate tectonics since the neoarchean. Geology 34, 961–964.

Gerya, T.V., Yuen, D.A., 2007. Robust characteristics method for modelling multiphase visco-elasto-plastic thermo-mechanical problems. Physics of the Earth and Planetary Interiors 163, 83 {105.

Taylor, S.R., McLennan, S.M., 1995. The geochemical evolution of the continental crust. Reviews of Geophysics 33, 241{265. Taylor.

P 1.8

3D fold growth rates

Frehner Marcel

Geological Institute, ETH Zurich, Sonneggstrasse 5, CH-8092 Zurich (marcel.frehner@erdw.ethz.ch)

Geological folds are inherently 3D structures. Therefore, a fold also grows in three dimensions (Bretis et al., 2011; Grasemann and Schmalholz, 2012). In this study, fold growth in all three dimensions is studied and quantified numerically using a finite-element algorithm for simulating 3D deformation of Newtonian materials. Upright symmetrical single-layer folds are considered. The higher-viscous layer exhibits a 2D Gaussian initial perturbation. Horizontal compression in x-direction leads to a folding instability, which grows from this perturbation in all three dimensions 1). Fold amplification in 3D setups has been described analytically by Fletcher (1991) for low limb dips, but fold growth in all three dimensions has not been quantified. It is described by:

Fold amplification (growth in z-direction):
Fold amplification describes the growth from a low-limb-dip fold to a higher-limb-dip fold.

Fold elongation (growth in y-direction):
Fold elongation is parallel to the fold axis. It describes the growth from a dome-shaped structure to a more cylindrical fold.

Sequential fold growth (growth in x-direction):
Sequential fold growth is parallel to the shortening direction and describes the growth of secondary (and further) folds adjacent to the initial isolated fold.

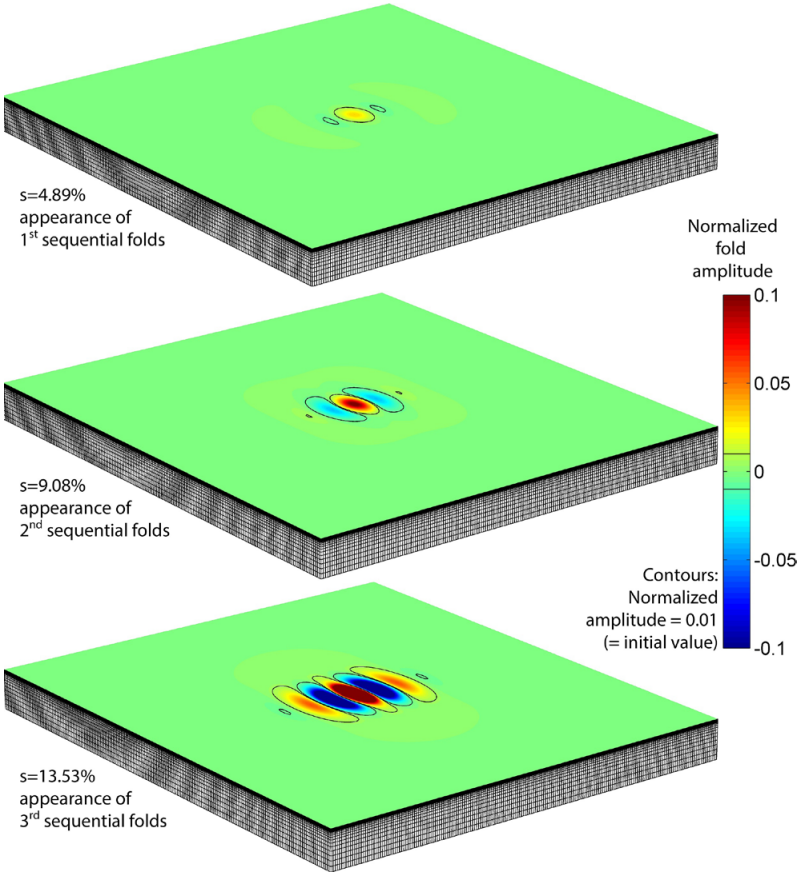

Figure 1: Growth of a 3D fold from a 2D Gaussian initial perturbation in all three dimensions.

Both fold elongation and sequential fold growth have previously been referred to as lateral fold growth, which is here used as an umbrella term for both.

The numerical results demonstrate that the two lateral directions generally show a very similar averaged growth (Figure 2). However, the fold elongation is smooth and continuous, while the sequential fold growth exhibits jumps in its evolution. These jumps occur whenever a secondary or further fold appears for the first time (1) and the entire fold structure therefore suddenly occupies more space in x-direction. For a given initial perturbation, the jumps occur earlier in the folding history for larger viscosity ratios.

Compared to the fold amplification, the two lateral directions grow slower (i.e., values <1 in Figure 2). Exceptions only occur for the sequential fold growth direction in early folding stages in the case of very narrow initial perturbations (Figure 2a). In these cases, the fold amplification is particularly slow and the sequential fold growth rate can therefore be larger. Generally, all three normalized fold amplitudes are of the same order (Figure 2), particularly at the early folding stages.

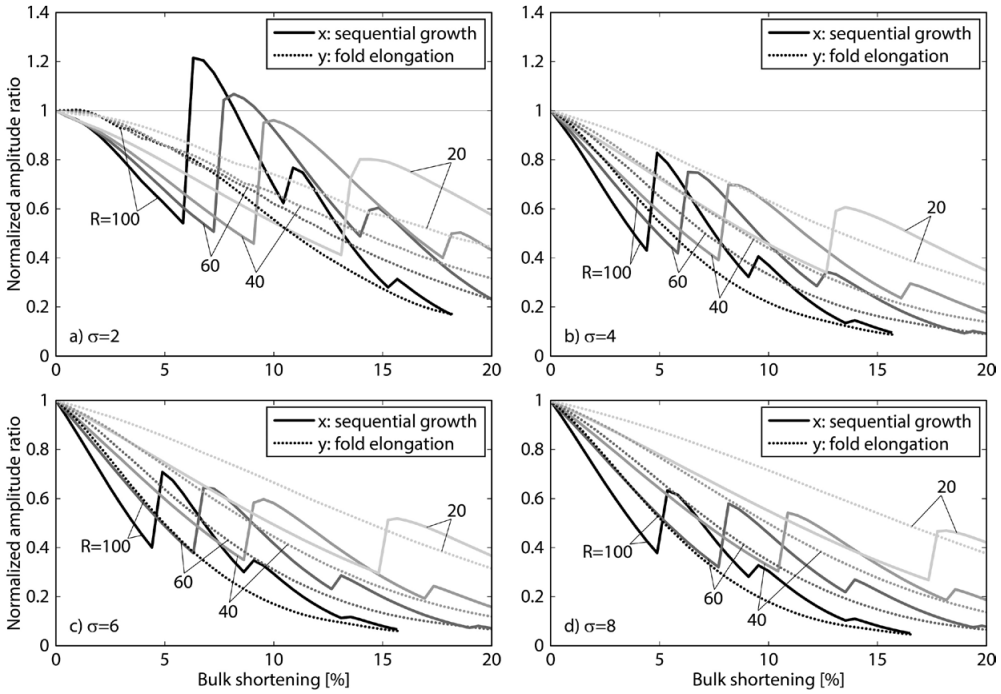

Figure 2. Ratios of normalized amplitudes *Ax*/*Az* (sequential growth/amplification, bold line) and *Ay*/*Az* (elongation/amplification, dotted line) for different initial perturbation widths (σ=2: narrow initial perturbation; σ=8: narrow initial perturbation) and different viscosity ratios $R=\eta_{layer}/\eta_{matrix}$. Values below 1 mean that the corresponding normalized lateral fold amplitude is smaller than the normalized vertical amplitude.

REFERENCES

Bretis, B., Bartl, N. and Grasemann, B. 2011. Lateral fold growth and linkage in the Zagros fold and thrust belt (Kurdistan, NE Iraq). Basin Research, 23, 615–630.

Grasemann, B. and Schmalholz, S. M. 2012. Lateral fold growth and fold linkage. Geology, 40, 1039–1042.

P 1.9

Towards coupled giant impact and long term interior evolution models

Golabek Gregor[1], Jutzi Martin[2], Gerya Taras[1] & Asphaug Erik[3]

[1] *Institut für Geophysik, ETH Zürich, Sonneggstrasse 5, CH-8092 Zürich (gregor.golabek@erdw.ethz.ch)*
[2] *Physikalisches Institut, Universität Bern, Sidlerstrasse 5, CH-3012 Bern*
[3] *School of Earth and Space Exploration, Arizona State University, 550 East Tyler Mall, AZ 85287, Tempe, USA*

The crustal dichotomy (McCauley et al., 1972) is the dominant geological feature on planet Mars. The exogenic approach to the origin of the crustal dichotomy (Wilhelms and Squyres, 1984; Frey and Schultz, 1988; Andrews-Hanna et al., 2008; Marinova et al., 2008; Nimmo et al., 2008) assumes that the northern lowlands correspond to a giant impact basin formed after primordial crust formation. However these simulations only consider the impact phase without studying the long-term repercussions of such a collision.

The endogenic approach (e.g. Weinstein, 1995), suggesting a degree-1 mantle upwelling underneath the southern highlands (Zhong and Zuber, 2001; Roberts and Zhong, 2006; Zhong, 2009; Keller and Tackley, 2009), relies on a high Rayleigh number and a particular viscosity profile to form a low degree convective pattern within the geological constraints for the dichotomy formation. Such vigorous convection, however, results in continuous magmatic resurfacing, destroying the initially dichotomous crustal structure in the long-term.

A further option is a hybrid exogenic–endogenic approach (Reese and Solomatov, 2006, 2010; Reese et al., 2010; Golabek et al., 2011), which proposes an impact-induced magma ocean and subsequent superplume in the southern hemisphere. However these models rely on simple scaling laws to impose the thermal effects of the collision.

Here we present the first results of impact simulations performed with a SPH code (Benz and Asphaug 1995, Jutzi et al., 2013) serially coupled with geodynamical computations performed using the code I3VIS (Gerya and Yuen, 2007) to improve the latter approach and test it against observations. We are exploring collisions varying the impactor velocities, impact angles and target body properties, and are gauging the sensitivity to the handoff from SPH to I3VIS.

As expected, our first results indicate the formation of a transient hemispherical magma ocean in the impacted hemisphere, and the merging of the cores. We also find that impact angle and velocity have a strong effect on the post-impact temperature field (e.g. Marinova et al., 2008) and on the timescale and nature of core merger.

REFERENCES

Andrews-Hanna J.C., Zuber M.T. and Banerdt W.B. 2008: Nature 453, 1212-1215.
Benz W. and Asphaug E. 1995: Computer Physics Communications 87, 253–265.
Gerya T.V. and Yuen D. A. 2007: Phys. Earth Planet. Int. 163, 83-105.
Golabek G.J., Keller, T., Gerya, T.V., Zhu G., Tackley P.J. and Connolly J.A.D. 2011: Icarus 215, 346-357.
Frey H. and Schultz R.A. 1988: Geophys. Res. Lett. 15, 229-232.
Jutzi M., Asphaug E., Gillet P., Barrat J-A. and Benz W. 2013: Nature 494, 207–210.
Keller T. and Tackley P.J. 2009: Icarus 202, 429-443.
Marinova M.M., Aharonson O. and Asphaug E. 2008: Nature 453, 1216-1219.
McCauley J.F., Carr M.H., Cutts J. A., Hartmann W.K., Masursky H., Milton D.J., Sharp R.P. and Wilhelms D.E. 1972: Icarus 17, 289-327.
Nimmo F., Hart S.D., Korycansky D.G. and Agnor C.B. 2008: Nature 453, 1220-1223.
Reese C.C. and Solomatov V.S. 2006: Icarus 184, 102-120.
Reese C.C. and Solomatov V.S. 2010: Icarus 207, 82-97.
Reese C.C., Orth C. P. and Solomatov V.S. 2010: J. Geophys. Res. 115, E05004.
Roberts J.H. and Zhong S. 2006: J. Geophys. Res. 111, E06013.
Weinstein S.A. 1995: J. Geophys. Res. 100, 11719-11728.
Wilhelms D.E. and Squyres S. W. 1984: Nature 309, 138-140.
Zhong S. 2009: Nature Geosci. 2, 19–23.
Zhong S. and Zuber M.T. 2001: Earth Planet. Sci. Lett. 189, 75-84.

P 1.10

3D Modeling of the Fribourg Area - Western Swiss Molasse Basin, Switzerland

GRUBER Marius[1], SOMMARUGA Anna[1], MOSAR Jon[1]

[1] *University of Fribourg, Departement of Geosciences, Earth Sciences, Chemin du Musée 6, CH-1700 Fribourg, Switzerland (marius.gruber@unifr.ch, anna.sommaruga@unifr.ch, jon.mosar@unifr.ch)*

This study focusses on the structural style of the western Swiss Molasse Basin (WSMB) near Fribourg (west of Bern, Switzerland). We are elaborating a 3D geological model with Move Software (Midland Valley) covering an area of 1700 km2 around the city of Fribourg. Based on 2D seismic line interpretations and deep borehole data (Sommaruga et al., 2012) three dimensional seismic horizons are built. Horizons correspond to the following stratigraphic boundaries: Near Base Tertiary, near Top Late Malm, near Top Early Malm, near Top Dogger, near Top Lias, near Top Trias, near Top Muschelkalk and near Base Mesozoic. Surface bed dip data from the Geological Atlas 1:25'000 (swisstopo) are included so as to improve orientations of geological strata. Fault surfaces in Tertiary and Mesozoic cover as well as in Pre-Mesozoic basement rocks are constructed based on seismic interpretations (Sommaruga et al. 2012), geological cross-sections (Geological Atlas 1:25:000, swisstopo) and hypocenter positions (Vouillamoz & Abednego, in prep.). Due to the lack of continuous seismic reflectors in Tertiary Molasse sediments, an appropriate mapping of fault structures in the latter is difficult. As a consequence Mesozoic fault surfaces are extrapolated through Tertiary Molasse sediments based on mapped surface fault structures (Geological Atlas 1:25'000, swisstopo; Ibele, 2011). 3D seismic horizons are depth converted based on a 3D heterogeneous P-velocity model of the Fribourg area (Abednego, in prep.).

The model shows a kinematic decoupling of Tertiary and Mesozoic units along a detachment horizon in Triassic evaporites. A second decoupling can be observed along the base Tertiary horizon in the south of the study area, probably linked to the thrust front of Subalpine Molasse as described in Ibele 2011. East of the city of Fribourg several N-S-striking, en echelon type normal faults in Mesozoic and Tertiary units can be observed. Faults form a zone of 20 km length. The zone is called the "Fribourg zone". Faults root in listric bends within middle Triassic evaporites forming a graben or half-graben structure. Triassic evaporites show an important thickening beneath the Fribourg zone. The location of fault traces between 2D seismic lines is speculative in the central part of the Fribourg zone due to a gap of seismic data. Recent studies on present earthquake activity show an enhanced recurrence of low magnitude earthquakes along the Fribourg zone. It is therefore proposed, that the Fribourg zone is formed by an assemblage of multiple small scale fault surfaces rather than a few large scale faults. The Fribourg zone forms the eastern border of a N-S striking, low amplitude syncline, called the "Fribourg structure". The N-S-alignment of the Fribourg structure deviates from the overall NE-SW trend of fold axis in the region. Triassic evaporites show a thinning beneath the Fribourg structure.

REFERENCES

IBELE, T. (2011). Tectonics of the Western Swiss Molasse Basin during Cenozoic Time, PhDThesis, University of Fribourg, 166 p.

SOMMARUGA, A., EICHENBERGER, U. and MARILLIER, F. (2012). Seismic Atlas of the Swiss Molasse Basin, Edited by the Swiss Geophysical Commission. Matér. Géol. Suisse, Géophys. 44.

P 1.11

Viscous overthrusting versus folding: 2-D quantitative modeling and its application to the Helvetic and Jura fold and thrust belts

Jaquet Yoann[1], Bauville Arthur[1], Schmalholz Stefan[1]

[1]*Institute of Earth Science, University of Lausanne, Bâtiment Geopolis, CH-1015 Lausanne (yoann.jaquet@unil.ch)*

This paper presents two-dimensional (2-D) numerical simulations of the shortening of a stiff viscous layer with pre-existing weak zones that is embedded in a weaker viscous matrix above a rigid detachment. Four deformation styles are observed that depend on the ratio of the layer and matrix viscosities, μ_L/μ_M; the ratio of the distance between the layer and the detachment to the layer thickness, H_M/H_L; and the power-law stress exponent of the matrix, n_M. The results show that (1) pure shear-dominated deformation occurs for μ_L/μ_M<~50 and n_M=1 (i.e., linear viscous); (2) overthrusting-dominated deformation occurs for n_M>1 (i.e., power-law viscous fluid), μ_L/μ_M>~50 and H_M/H_L<~0.5; (3) folding-dominated deformation occurs for n_M=1, μ_L/μ_M>~50, and H_M/H_L>~1; and (4) folding and overthrusting occur for n_M>1 and ~0.5<H_M/H_L<~2. The power-law stress exponent of the stiff layer has a minor effect on deformation style. Simulations with layers that contain two weak zones show the formation of a nappe stack. The change in deformation style as a function of H_M/H_L corroborates field observations from the Helvetic nappe system. The agreement of the results with first-order observations from the Helvetic fold and thrust belt suggest that ductile deformation dominated this fold and thrust belt.

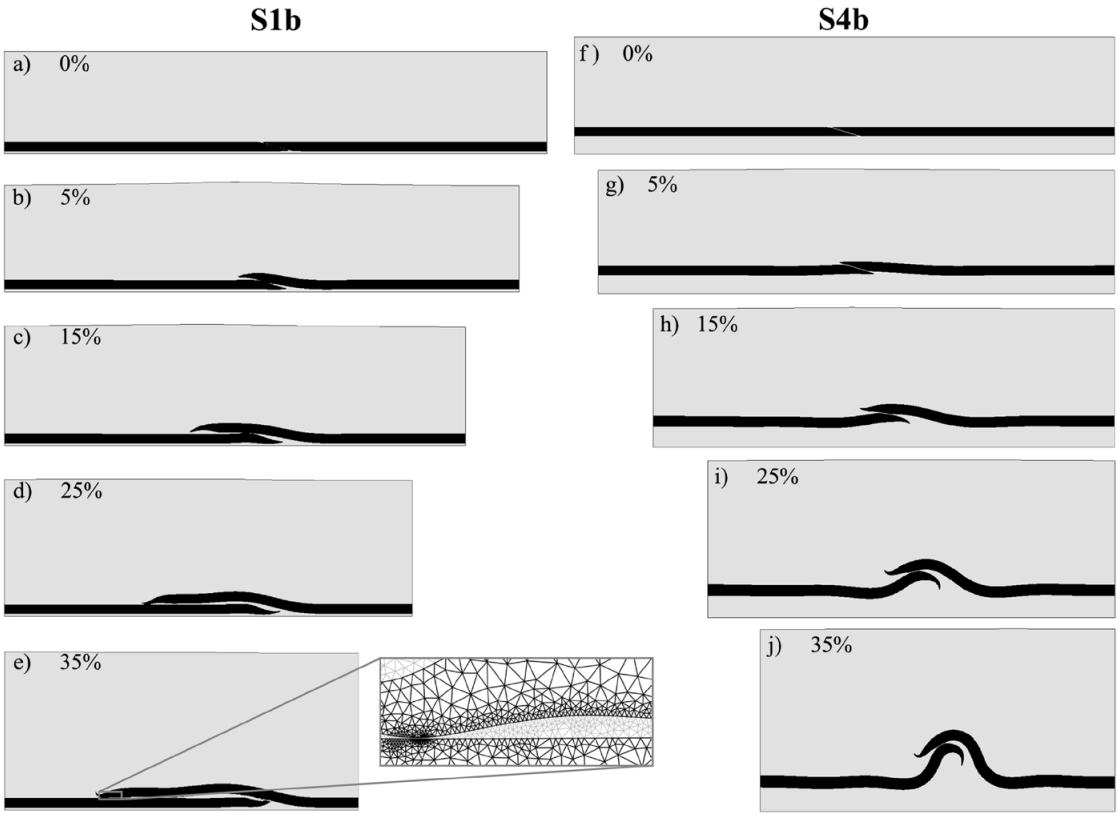

Figure 1: The development of the model geometry with increasing shortening. The layer (black) is linear viscous, whereas the matrix (gray) is power-law viscous (n_M=5). a-e) The model has a viscosity ratio (μ_L/μ_M) of 200 and a thickness ratio (H_M/H_L) of 0.25. During shortening, the layer deforms by essentially overthrusting. f-j) The model has a viscosity ratio (μ_L/μ_M) of 100 and a thickness ratio (H_M/H_L) of 1. During shortening, the layer deforms by simultaneously overthrusting and folding. The detail of the numerical mesh is shown in e).

P 1.12

Mapping Earth's interiors with GPS records: the first steps.

Kelevitz Krisztina[1],[2], Houlie Nicolas[1],[2] , Rothacher Markus[2], Giardini Domenico[1]

[1] *Institute of Geophysics, ETH Zurich, Switzerland*
[1] *Institute of Geodesy and Photogrammetry, ETH Zurich, Switzerland*

Nowadays, GPS networks are expanding faster than the global network of broadband seismometers (STS-1 or STS-2). Indeed, almost 10.000 GPS receivers are recording data at 1 Hz with 100+ stations are streaming data in Real-Time (RT). The reasons for this quick expansion are the price of receivers, their low maintenance, and the wide range of activities they can be used for (transport, science, public apps, etc.).

Many authors proposed then that GPS could help studying not only the long-term continuous continental deformation (earthquake sources [Cervelli, et al., 2001; Langbein et al., 2006], volcanoes [Houlié, et al., 2006a], post seismic deformation [Langbein et al., 2006]) but also transient (less than one hour) ground deformation [Houlié et al., 2011]. Potential applications are numerous including seismic wave propagation at the regional or global scale and earthquake source studies.

In this poster we are presenting work completed on the GPS records of the Hokkaido earthquake (2003 September 25th, Mw=8.3). 1Hz GPS waveforms have been recomputed by improving the inversion of the ground motion displacement history. GPS are computed in the range of frequencies 0.02-0.033 Hz and 0.002-0.033 Hz; the latter frequency band matching the frequency range recorded by a very-broadband STS-1 seismometer (up to 300s with flat response).

At co-located sites (STS-1 and GPS located within 10km) the agreement is good for the vertical component. We show that 1) horizontal components are dependent on the distribution of the satellites visible in the sky at the moment of the seismic wave front propagation while 2) the new inversion algorithm improves the accuracy of the east component of the GPS data.

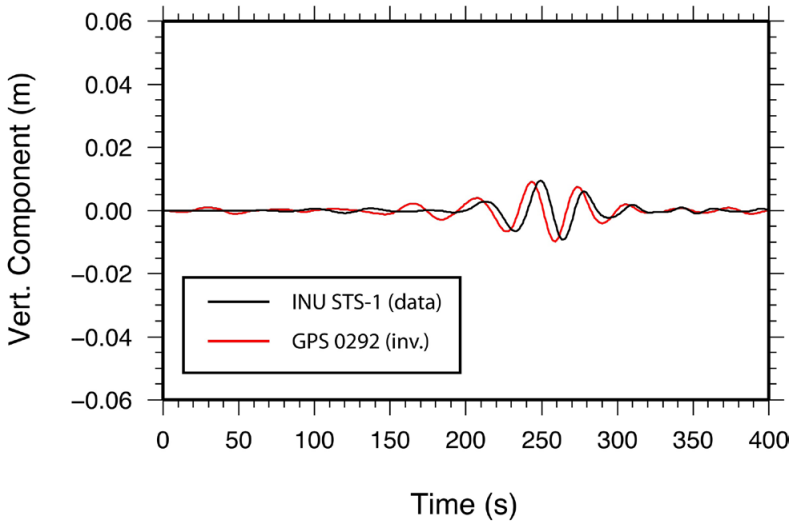

Figure 1: We compare the time-series of GPS displacement (in red) with the seismograms recorded at the GEOSCOPE site INU (in black). We note that while the agreement between the two sets of waveforms is reasonable for vertical component. Instrument responses have been provided by GEOSCOPE. Both datasets have been band-pass filtered between 30 and 50 seconds (20 and 35 mHz) according to the periodogram presented in Figure 5. From Houlié et al., 2011

REFERENCES

Cervelli, P. et al. 2001: Estimating source parameters from deformation data, with an application to the March 1997 earthquake swarm off the Izu Peninsula, Japan

Houlié, N., et al. 2006a: Large scale ground deformation of Etna observed by GPS between 1994 and 2001

Houlié, N., et al. 2011: New approach to detect seismic surface waves in 1Hz-sampled GPS time series

Langbein, J., et al. 2006: Coseismic and initial postseismic deformation from the 2004 Parkfield, California, earthquake, observed by global positioning system, electronic distance meter, creepmeters, and borehole strainmeters

P 1.13

The role of phase distribution and reaction in an amphibolite facies ultramylonite

Kilian Rüdiger

Geological Institute, Basel University, Switzerland, Bernoullistr. 32, 4056 Basel, (ruediger.kilian@unibas.ch)

Rocks deforming by diffusion creep are usually characterized by a small grain size, an anti-correlated phase distribution and the lack of a crystallographic preferred orientation. The present study focuses on the role of bulk material transfer and reaction during homogeneous flow of an amphibolite facies ultramylonite.

The analyzed samples are from the Nordmannvik Nappe, Upper Allochton of the Norwegian Caledonides. The shear zone separates a marble unit from a garnet amphibolite with enclosed relict mafic granulite lenses. Contacts with the wallrock are very sharp and no intermediately strained zone is present.

The ultramylonite matrix is composed of quartz, biotite, white mica, oligoclase and ilmenite with grain sizes below 10 µm (eq. diameter) and has an extremely homogeneous microstructure. Grains have slightly lobate, interlocking boundaries. Aligned grain and phase boundaries are absent and shear bands are very rare.

Garnet, white mica and plagioclase-quartz aggregates form porphyroclasts. Towards the center of the shear zone, porphyroclasts disappear subsequently while garnet porphyroclasts are the last being present. The increase in matrix percentage from 80 to 98% is interpreted to result from increasing strain. White mica and plagioclase-quartz porphyroclasts attain aspect ratios of 2-3 while garnet remains at low aspect ratios. White mica porphyroclasts have monoclinic shapes and a stable orientation of the clast long axis at 5° with respect to the lineation, which is independent on strain and clast size. Plagioclase porphyroclasts have orthorhombic shapes and reach a stable orientation less frequently.

The matrix shows a strong anti-correlation of quartz clusters and biotite and white mica. Quartz clusters are separated by biotite stacks parallel to the foliation and by white mica perpendicular to the foliation. Those quartz clusters have a long axis at 50 -70° to the foliation, inclined against the sense of shear. Occasionally thin Fe-Ca-rich seams decorate quartz grain boundaries which are oriented at a low angle to the foliation.

Adjacent to porphyroclasts, the matrix homogeneity is locally disturbed. In the sector of instantaneous shortening around porphyroclasts, matrix biotite and plagioclase are depleted and garnet shows newly grown seams. In the sectors of instantaneous stretching, biotite and plagioclase grow and occasionally garnet porphyroclasts show signs of dissolution. Within less than 1mm, the homogeneity of the matrix is reestablished. Foliation parallel biotite is replaced by white mica during thinning of the mica aggregates and concurrently biotite grows adjacent to quartz grains in stacks perpendicular to the foliation. The anti-correlation of oblique quartz clusters and mica is the result of both processes.

The microstructures suggest that dissolution, replacement, nucleation and growth of matrix phases occur synkinematically and simultaneously. A cyclic reaction of garnet + white mica = plagioclase + biotite, driven by local gradients, can explain the observations.

P 1.14

Offsetting crustal and mantle neckings generates abandonment of continental rifts

Liao Jie[1], & Gerya Taras[1]

[1] *Geophysical Fluid Dynamics, Institute of Geophysics, ETH Zurich, Zurich, Switzerland (jie.liao@erdw.ethz.ch)*

During continental extension, localized deformation can redistribute, and as a consequence, a new continental rift is generated offsetting from the previously formed rift that is abandoning. This phenomenon is called continental rifts jump, and the natural examples of continental rifts jump are globally distributed (Wood, 1983, Armitage et al., 2010, Yamasaki and Gernigon, 2010). The reasons why continental rifts jump remain elusive. Once deformation initiates in a pre-existing weakness (Dunbar J. A., 1988), whether deformation will concentrate in this area or migrate to a new location is determined by the competition between thermal diffusion (lithosphere strengthening) and thermal advection (litho- sphere weakening) (Buck et al., 1999, Yamasaki and Gernigon, 2010). Slow extension corresponds to slow thermal advection and fast thermal diffusion, which favors lithosphere strengthening (England, 1983), and may generate the abandonment of intracratonic rifts (White, 1999). Numerical models suggest that the multi-phase rifting history [Armitage et al., 2010], migration of plume or thermal event (such as magma intrusion) (Yamasaki and Gernigon, 2010) are possible mechanisms that leads to the redistribution of deformation during extension.

Here, based on three-dimensional thermo-mechanical numerical models, we demonstrate that the formation of offsetting crustal and mantle neckings leads to the abandonment of continental rifts. Offsetting crustal and mantle neckings are naturally formed in the model employing crust-mantle- decoupled rheology and a crustal weak zone. Crustal weak zone controls the formation of the crustal necking and the initial continental rift in the early extension stage. Decoupled rheology determines the formation of mantle necking after a certain extension, which is offsetting from the crustal necking. The offsetting mantle necking becomes dominate and therefore governs a new continental rift development (from rifting, breakup to seafloor spreading), and as a consequence, the initial continental rift is abandoned.

REFERENCES

Armitage, J. J., Collier, J. S., & Minshull, T. A. 2010:The importance of rift history for volcanic margin formation. Nature 465, 913–917.

Buck, W. R., Lavier, L. L., & Poliakov, A. N. B. 1999: How to make a rift wide. Phil. Trans. R. Soc. Lond. A 357, 671–693.

Dunbar, J. A., & Sawyer, D. S. 1988: Continental rifting at pre-existing lithospheric weaknesses. Nature 333, 450–452.

England, P. 1983: Constraints on extension of continental lithosphere. J. Geophys. Res. 88(B2), 1145–1152.

White, R. S. 1999: The lithosphere under stress. Phil. Trans. R. Soc. Lond. A 357, 901–915.

Wood, C. A. 1983: Continental rift jumps. Tectonophysics 94, 529–540.

Yamasaki, T., & Gernigon, L. 2010: Redistribution of the lithosphere deformation by the emplacement of underplated mafic bodies: implications for microcontinent formation. Journal of the Geological Society, London 167, 961–971.

P 1.15

Deformation of the Sumatran, Chilean, and Japanes volcanic arcs after mega-thrust slips

Lupi, M.[1] , Saenger. E.H.[1], Fuchs, F.[2], Miller, S.A.[2]

1 ETH Zurich, Geological Institute, Sonnegstrasse 5, 8092, Zurich, CH
[2] Steinmann Institute, University of Bonn, Meckenheimer Allee 173, Bonn, DE

Eruptive rates in volcanic arcs increase significantly after subduction zone mega-thrust earthquakes. Over short time periods the response of the volcanic arc is attributed to the passage of seismic waves and almost-instantaneous subsidence of the volcanic system. A second peak of activity also occurs over decadal timescales but a kinematic mechanism that controls long-term pulses has yet to be proposed.

We conducted Coulomb stress transfer analyses to investigate the stress perturbations induced by five recent mega-thrust earthquakes (2005 M8.6, 2007 M8.5, and 2007 M7.9 Sumatra earthquakes; the 2010 M8.8 Maule, Chile earthquake; and the 2011 M9.0 Tohoku, Japan earthquake) and compared them with (large magnitude) shallow seismic activity occurring in the years that followed the mega-thrust slip. We use geomechanical, geological, and geophysical arguments to suggest that increased volcanic activity over longer timescales is due to a change of the local kinematics in the arc. More specifically, our study highlights a relaxation of the compressional regime that accompanies mega-thrust subduction zone earthquakes, which in turn promotes the reduction of the horizontal stress σh. This causes the occurrence of short-lived strike-slip kinematics and facilitates magma mobilization. Our results show that all, but one, the shallow earthquakes that occurred in the arcs of Sumatra, Chile and Japan have a marked lateral component. We suggest that the long-term volcanic response of the Sumatran, Chilean, and Japanse volcanic arcs will be manifested as predominantly strike-slip seismic events, that will be followed closely by seismic swarms, inflation, and other indications of a rising magma source.

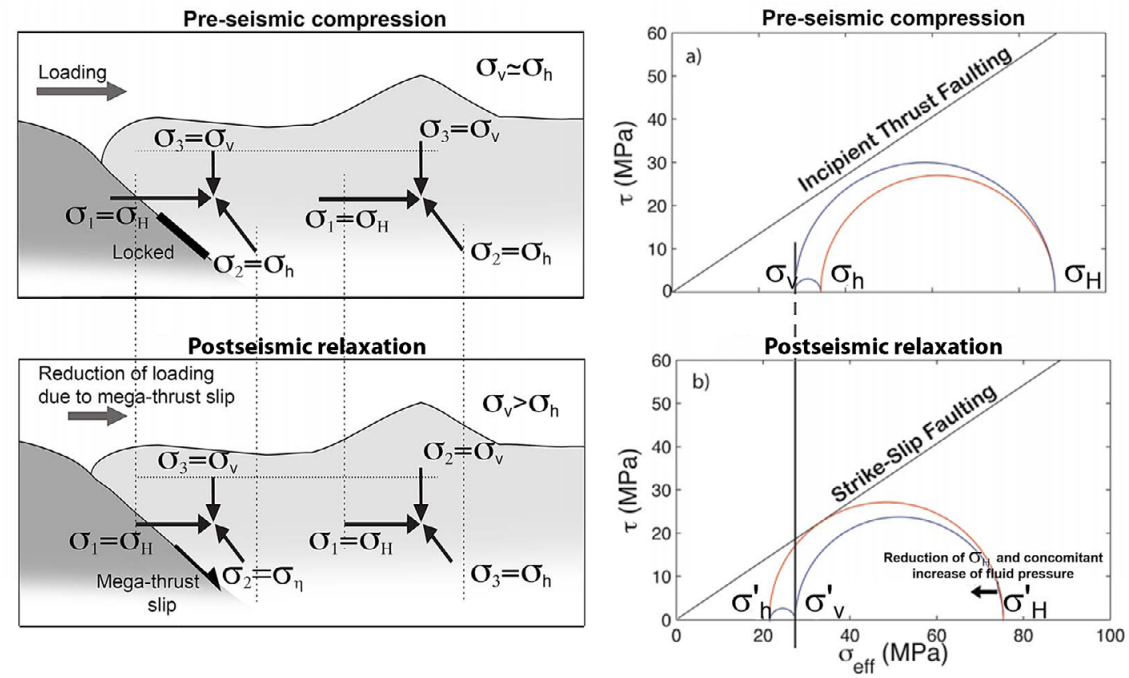

P 1.16

Tectonic events predating the formation of the Jura fold-and-thrust belt: Constraints from cross section balancing

Malz Alexander[1], Jordan Peter[2], Meier Beat[3], Madritsch Herfried[4], Navabpour Payman[1] & Kley Jonas[5]

[1] *Institute of Geosciences, Friedrich-Schiller-University Jena, Burgweg 11, D-07749 Jena (alexander.malz@uni-jena.de)*
[2] *Böhringer AG, Mühlegasse 10, CH-4104 Oberwil*
[3] *Proseis AG Zürich, Schaffhauserstrasse 418, CH-8050 Zürich*
[4] *Nagra, Hardstraße 73, CH-5430 Wettingen*
[5] *Georg-August-Universität Göttingen, Geowissenschaftliches Zentrum, Goldschmidtstr. 3, D-37077 Göttingen*

The deformation of the Jura fold-thrust-belt in the foreland of the Western Alps is widely accepted to be of a thin-skinned type (Laubscher 1961). Most folds and thrusts are considered to have been formed above a subhorizontal basal detachment (décollement) located in Middle to Upper Triassic evaporites. Especially, in the easternmost part of the Jura Mountains this décollement and the underlying pre-Mesozoic basement is locally dissected by Palaeozoic normal faults that were reactivated during the Tertiary subsidence of the Molasse basin (Diebold & Noack 1997). During the Mesozoic, the area of the future Jura fold-thrust-belt is widely considered to have witnessed a time of relative tectonic quiescence. This general view contrasts with sedimentological indications for differential subsidence (Allenbach 2002) and large scale analyses of the North-Alpine foreland (Ziegler 1990). The latter suggest extensional deformation during Jurassic up to Cretaceous times and a phase of transtension and compression during the Upper Cretaceous and Early Cenozoic.

Here we present a new interpretation of a recently reprocessed and depth migrated seismic reflection profile across the eastern Jura, which incorporates all available geological field and subsurface data and was verified by classical cross section balancing methods of equal bed length and constant area. Beside the restoration of the thin-skinned thrust stack we also explore the probable pre- thrusting tectonic evolution along the section.

Our results reveal thickness changes of Jurassic strata that could point toward a Middle Jurassic extensional deformation event. Moreover, thickness variations between the base of the Upper Jurassic and the discordance of the base of the Tertiary may suggest a second, contractional deformation event during Cretaceous-Palaeocene times, coinciding with a phase of transpression in the North Alpine foreland (Ziegler 1987) and erosion of up to 700 m of Cretaceous strata prior to the Molasse sedimentation (Mazurek et al. 2006).

REFERENCES

Allenbach, R.P. 2002: The ups and downs of "Tectonic Quiescence" - recognizing differential subsidence in the epicontinental sea of the Oxfordian in the Swiss Jura Mountains. Sedimentary Geology, 150, 323-342

Diebold, P. & Noack, T. 1997: Late Paleozoic troughs and Tertiary structures in the eastern Jura. In: Heitzmann, P. & Lehner, P. (eds.): Deep structures of the Swiss Alps. Birkhäuser Verlag, Basel.

Laubscher, H. 1961: Die Fernschubhypothese der Jurafaltung, Eclogae Geol. Helv., 54, 222 – 282.

Mazurek, M., Hurford, A.J. & Leu, W. 2006: Unravelling the multi-stage burial history of the Swiss Molasse Basin: Integration of apatite fission track, vitrinite reflectance and biomarker isomerisation analysis, Basin Research, 18, 27-50.

Ziegler, P.A. 1987: Late Cretaceous and Cenozoic intra-plate compressional deformation in the Alpine Foreland – a geodynamic model, Tectonophysics, 137, 389-420.

Ziegler, P.A. 1990: Geological Atlas of Western and Central Europe. Shell Internationale Petroleum Maatschappij, Den Haag.

P 1.17

Semi-brittle deformation of fault rocks - an experimental study of the brittle-to-viscous transition in mafic rocks

Sina Marti[1], Renée Heilbronner[1], Holger Stünitz[2]

[1] *Department of environmental sciences, Geological institute, University of Basel, Bernoullistr. 32, 4056 Basel (sina.marti@unibas.ch)*
[2] *Department of Geology, University of Tromso, Dramsveien 201, Tomso Norway*

In order to investigate the brittle-viscous transition in mafic rocks, a series of rock deformation experiments is carried out – here we report the first results.

The experiments are performed using a modified Griggs-type solid-medium apparatus at confining pressures of Pc = ~0.5 GPa and ~1.0 GPa, temperatures, T, between 300°C and 700°C and shear displacement rates of d = $\sim 10^{-8}$ ms^{-1} and $\sim 10^{-7}$ ms^{-1} along the 45° precut (inducing shear strain rates of $\gamma = \sim 10^{-5}$ s^{-1} and $\sim 10^{-4}$ s^{-1} in the fault rock). The starting material is crushed Maryland diabase sieved to a grain size <125 µm, with a composition of ~ 57% Plg, 33% Cpx, 8% Opx, and 2% accessories (apatite, Kfs, Qtz, ilmenite, magnetite and biotite).

The peak stress, τ_{max}, and the steady state shear stress, τ_{flow} of the fault rock show both a temperature and a pressure dependence:

- At confining pressures, of ~1 GPa and T=300°C, $\tau_{max} \approx 1.4$ GPa and $\tau_{flow} \approx 1.2$ GPa; at T=700°C, $\tau_{max} \approx 0.7$ GPa and $\tau_{flow} \approx 0.6$ GPa.
- At confining pressures, of ~0.5 GPa and T=300°C, $\tau_{max} \approx 1.1$ GPa and $\tau_{flow} \approx 1.05$ GPa; at T=700°C, $\tau_{max} \approx 0.5$ GPa and $\tau_{flow} \approx 0.25$ GPa.

At Pc = ~0.5 GPa and d = $\sim 10^{-8}$ ms^{-1}, the stress-strain curves show the same initial slope for all T. With increasing shear stress, τ, the curves start to deviate from the initial slope indicating the beginning of yielding with a lower slope until peak stress values, τ_{max}, are reached. After the τ_{max}, the rocks weaken to a steady state shear stress, τ_{flow} Despite the initial congruency of the stress-strain curves at all temperatures, the shear stresses at yielding and the peak stresses decrease with increasing T.

Microstructural observations show that at T=300°C, a strong foliation develops due to the formation of pervasive micro shear-fractures in Riedel shear orientation. Prominent slip-zones of approx. 10 to 20 µm in thickness form; they contain highly comminuted material and display flow structures and small scale folding. With increasing T, micro-fracturing decreases and the slip-zones become less prominent. At T > 500°C, solution and precipitation microstructures are observed, like the dissolution of Ca-depleted exsolution lamellae in pyroxene and healing of fractures in plagioclase and more Ca-rich pyroxene.

So far we conclude that the dominating processes that accumulate strain are fracturing and granular flow. The pressure dependence of strength is interpreted to indicate the influence of friction on deformation. The strong sensitivity to temperature is not yet well understood and needs further investigations.

P 1.18

A scalable, parallel matrix-free Stokes solver for geodynamics applications

Dave A. May[1]

[1] *Institute of Geophysics, ETH Zurich, Sonneggstrasse 5, CH-8092 Zurich (dave.may@erdw.ethz.ch)*

Here I describe a numerical method suitable for studying non-linear, large deformation processes in crustal and lithospheric dynamics. The method utilizes a hybrid spatial discretisation which consists of mixed finite elements for the Stokes flow problem, coupled to a Lagrangian marker based discretisation to represent the material properties (viscosity and density). This approach is akin to the classical Marker-And-Cell (MAC) scheme of Harlow and the subsequently developed Material Point Method (MPM) of Sulsky and co-workers. The geometric flexibility and ease of modelling large deformation processes afforded by such mesh-particle methods has been exploited by the lithospheric dynamics community over the last 20 years.

The strength of the Stokes preconditioner fundamentally controls the scientific throughput achievable and represents the largest bottleneck in the development of our understanding of geodynamic processes.

The possibility to develop a "cheap" and efficient preconditioning methodology which is suitable for the mixed Q2-P1 element is explored here. I describe a flexible strategy, which aims to address the Stokes preconditioning issue using an upper block triangular preconditioner, together with a geometric multi-grid preconditioner for the viscous block. The key to the approach is to utilize algorithms and data-structures that exploit current multi-core hardware and avoid the need for excessive global reductions. In order to develop a scalable method, special consideration is given to; the definition of the coarse grid operator, the smoother and the coarse grid solver.

The performance characteristics of this hybrid matrix-free / partially assembled multi-level preconditioning strategy is examined. The robustness of the preconditioner with respect to the viscosity contrast and the topology of the viscosity field, together with the parallel scalability is demonstrated.

P 1.19

Detrital zircon and provenance analysis on the onshore Makran accretionary wedge, SE Iran: implication for the geodynamic setting

Mohammadi Ali[1], Winkler Wilfried[1], Burg Jean-Pierre[1], Ruh Jonas[1], Von Quadt Albrecht[1]

[1] *Geological Institute, ETH-Zurich, Sonneggstrasse 5, CH- 8092 Zürich*

The Makran, located in Southeast Iran and South Pakistan, is one of the largest accretionary wedges on Earth. In Iran it comprises turbiditic sediments ranging in age from Late Cretaceous to Holocene. We present a provenance analysis on sandstones, which is aimed at reconstructing the assemblages of source rocks and the tectonic setting from which the clastic material was derived. Sandstone samples collected from different units span the regional stratigraphy from Late Cretaceous to Miocene.

Laser ablation ICP-MS resulted in ca 2800 new U-Pb ages of individual detrital zircons from 18 samples collected in onshore Makran. 101 detrital zircons from a Late Cretaceous fine grained sandstone range from 180 to 160 Ma (Middle Jurassic). 478 detrital zircons from mid- to late Eocene sandstones allow differentiating a NE and NW sector of the Makran Basin. Zircon grains in the NE basin belong to two populations peaking at 180 to 160 Ma (late Early to Middle Jurassic) and 50 to 40 Ma (Mid-Eocene), with the noticeable absence of Cretaceous grains. In the NW basin, detrital zircons are 120 to 40 Ma (late Early Cretaceous to Lutetian, Eocene). 587 detrital zircon grains from fine to medium grained Oligocene sandstones collected over the whole area also range from 120 to 40 Ma (late Early Cretaceous to Eocene, Lutetian). 1611 detrital zircons from early Miocene sandstones show again distinctly different ages in the eastern and western parts of the basin. They range from 120 to 40 Ma (late Early Cretaceous to Eocene) in the eastern and from 80 to 40 Ma (Late Cretaceous to Eocene) in the western basin.

Hf isotopes analyses were performed on 120 zircon grains from 6 samples. Negative values (-2 to -15) in Middle Jurassic and late Early Cretaceous zircons indicate minor or no influence of mantle reservoirs which implies a rifting setting during crystallization of the zircons. Low negative to positive (-5 to +10) values in Late Cretaceous and Eocene zircons indicate mixed crustal and juvenile magma sources, which are common in continental arc environments.

Point counts of 32 sandstone thin sections were performed following the Gazzi-Dikinson method. 300-400 points were counted in each thin section. The sandstones are feldspathic litharenites and litharenites. Feldspar is dominantly plagioclase (> 90%) with minor amounts of K-feldspar. Most quartz grains (75%) are mono-crystalline but poly-crystalline ones (maximum 25%) occur. Rock fragments are represented by sedimentary, volcanic and metamorphic grains. Volcanic rock-fragments mostly are andesites and volcanic chert. Sedimentary lithic grains comprise mostly sandstone, siltstone, limestone and dolomite. Metamorphic lithic grains generally are low-grade schists and phyllites. In various compositional ternary diagrams, the sources of the sandstones plot in the transitional to dissected arc and recycled orogenic fields.

We selected 26 samples for heavy mineral study. 200-300 grain were identified and counted in each sample. Heavy mineral suites show a highly variable composition including (1) a group of ultra-stable minerals (zircon, monazite, tourmaline, rutile, brookite, anatase and sphene) derived from a granitic continental crust sources, (2) metastable minerals delivered from variable metamorphic-grade source rocks (epidote group, garnet, staurolite, chloritoid, kyanite, andalusite, glaucophane), (3) chromian spinel from ultrabasic rocks, (4) common hornblende either supplied from metamorphic or basic igneous series, and (5) a local pyroxene-rich source in the pyroclastic sandstone formation overlying pillow lavas. Glaucophane (5-20%) occurs in several samples, which indicates high-pressure/low-temperature metamorphic rocks in the detrital source areas for Eocene and Miocene sandstones.

Earlier work in the Pakistani Makran suggested that pre-Miocene sediments were supplied from the Himalaya, whereas Miocene to Recent deposits were reworked older sediments of the accretionary wedge. Our data do not support this conclusion. Instead, we identified rifting-related detrital sources from Middle Jurassic to late Early Cretaceous (175 - 100 Ma) and the establishment of a continental volcanic arc from Late Cretaceous to Eocene (80 to 40 Ma). In addition, paleocurrent directions in Makran sandstone show general sediment transport from North to South; Cr-spinel as well as high-P/low-T heavy minerals most likely have been derived from the blueschist-bearing Makran ophiolitic and igneous belt to the North.

P 1.20

Metamorphic conditions and exhumation of the Keshebir-Kardamos dome – Rhodope Metamorphic Complex (Greece-Bulgaria)

Moulas Evangelos[1], Burg Jean-Pierre[1], Kostopoulos Dimitrios[2], Schenker Filippo[1] & Chatzitheodoridis Elias[3]

[1] *Department of Earth Sciences, ETH-Zurich, Sonneggstrasse 05, CH-8092 Zurich (evangelos.moulas@erdw.ethz.ch)*
[2] *Department of Mineralogy and Petrology, University of Athens, Panepistimioupoli Zographou, 15784, Athens, Greece*
[3] *School of Mining and Metallurgical Engineering, National Technical University of Athens, Heroon Polytechniou 9, 15780, Athens, Greece*

The Rhodope Metamorphic Complex (RMC) in northern Greece and southern Bulgaria is a synmetamorphic nappe pile that developed during the Alpine-Himalayan orogen. The nappe system is deformed and forms dome-and-basin structures that indicate syn- to post-convergent exhumation. High-pressure rocks showing variable degrees of retrogression occur in the intermediate imbricate units including eclogites and micro-diamond-bearing paragneisses. We document the deformation style and present new thermobarometric and geochronological constraints for the Keshebir-Kardamos dome in the eastern RMC in an attempt to comprehend the major mechanisms involved in the exhumation of high-pressure (HP) and high-temperature (HT) rocks.

The studied high-grade metamorphic rocks from the intermediate thrust sheets of the core of the Kardamos dome are broadly subdivided into two compositional groups: a) typical Ca-poor pelites and b) calcsilicate lithologies. For the Ca-poor compositions, thermodynamic modelling using phase diagram sections in the NCKFMMnASHT (Na_2O-CaO-K_2O-FeO-MgO-MnO-Al_2O_3-SiO_2-H_2O-TiO_2) model system suggests peak conditions at 1.2 GPa and ca. 750°C. Garnet-clinopyroxene thermometry combined with Raman barometry applied on quartz inclusions in garnets from the calcsilicate lithologies corroborate the above calculations within 0.1GPa (i.e. 1.3 GPa and ca. 750°C). Thin chlorite and biotite selvedge replacing garnets along cracks and minor albite replacing more calcic plagioclase document minor greenschist-facies retrogression. U-Pb SHRIMP dating of zircons from the metapelites reveals Early Cretaceous (144 Ma) as the time of the major metamorphic overprint whereas some zircon rims yield reset ages at Eocene times (53 and 44 Ma).

Kinematic indicators from the imbricate units suggest a continuum from ductile to brittle conditions during exhumation. The exhumed high-grade rocks were covered by marine sediments soon after their exhumation (Lutetian-Priambonian?). Slumps in sediments suggest that sedimentation took place in a tectonically active environment. Our new structural, petrological and geochronological data suggest that the major shear zone in the core of the Keshebir-Kardamos dome is equivalent to the Nestos-Chepelare suture zone.

P 1.21

Assessment of mercury distribution in sediments, soil, fish and human hair sampled in gold mining areas in the Gambia River Basin at Kedougou, southeastern Senegal

Niane Birane[1], Moritz Robert[1], Guédron Stéphane[2], Poté John[1], Ngom Papa Malick[3], Pfeifer Hans Ruedi[4]

[1] *Section des sciences de la Terre et de l'Environnement, Université de Genève, Rue des Maraîchers 13, 1205 Genève*
[2] *Institut des sciences de la Terre Université Joseph Fourier, F-38041, Grenoble, France*
[3] *Département de géologie, Université de Cheikh Anta DIOP, Dakar, Sénégal*
[4] *Institut des sciences de la Terre, Université de Lausanne, Géopolis 3871, Lausanne*

Little information is available on the impact of mercury (Hg) from artisanal small-scale gold mining (ASGM) in environmental compartments, and neither is there much information regarding the assessment and potential impact of Hg in biota and human health in Sub-Saharan Africa, especially in the Kedougou region, southeastern Senegal.

The Kedougou inlier is interpreted as an accretion of north-easterly trending Birimian age volcanic terrains. There are two types of gold mineralization: alluvial gold and gold-bearing quartz veins hosted by shear zones. Approximately 30,000-60,000 persons are involved since about 1995 in ASGM activities spread across several villages. This study has been under-

taken to assess the impact of ASGM in different sites of the Kedougou region. The assessment was based on the determination of Hg contents in sediment and soil profiles, in various fish species and human hairs collected in the region.

The total Hg (THg) concentration from different samples was obtained using an AMA-254 mercury analyzer (Atomic Absorption Spectrometry). The accuracy of measurements was checked by analyzing the reference material MESS- 3 (National Water Research Institute, Canada) in between every third sample. Enrichment factors were used to classify the sampling sites according to their degree of contamination.

The results indicate that sediments and soils from the active ASGM sites have high levels of THg in contrast to reference sites. The comparison of THg sediment concentrations at different sites with the values of sediment quality guideline shows that the main active ASGM sites present concentrations of Hg higher than standard recommended values. The THg concentrations range from 0.14 to 1.6 mg/kg in fish species, exceeding WHO standard recommendations of 0.5 mg/kg in piscivorous fish. THg concentrations in hair range between 0.10 and 7.67 mg/kg, with 5 mg/kg being the maximum concentration recommended by WHO. The results of this study demonstrate that ASGM in the Kedougou region are potential environmental and human hazards.

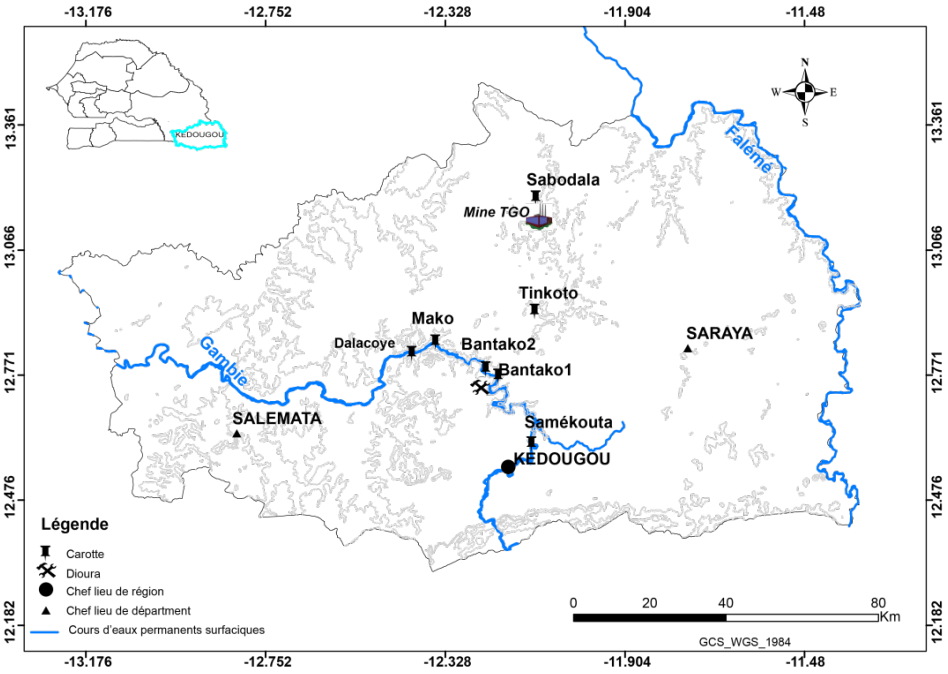

Figure 1: Sampling locations in the Kedougou study area eastern Senegal

REFERENCES

Bassot, J. P. (1997). Albitisations dans le Paléoprotérozoïque de l'Est du Sénégal: relations avec les minéralisations ferrifères de la rive gauche de la Falémé. Journal of African Earth Sciences 25: 353-367.

Donkor, A. K. et al. (2006). Mercury in different environmental compartments of the Pra River Basin, Ghana. Science of The Total Environment 368: 164-176.

Kainz, M. and M. Lucotte (2002). Can flooded organic matter from sediments predict mercury concentrations in zooplankton of a perturbed lake? Science of The Total Environment 293: 151-161.

Katner, A., et al. (2010). An evaluation of mercury levels in Louisiana fish: Trends and public health issues. Science of The Total Environment 408: 5707-5714.

MacDonald, D. D. et al. (2000). Development and Evaluation of Consensus-Based Sediment Quality Guidelines for Freshwater Ecosystems. Archives of Environmental Contamination and Toxicology 39: 20-31.

van Straaten, P. (2000). Mercury contamination associated with small-scale gold mining in Tanzania and Zimbabwe. The Science of The Total Environment 259: 105-113.

P 1.22

Single Viscous Layer Fold Interplay And Linkage: A 3d-Fem Modelling Approach

Philippe Thomas A.[1], Frehner Marcel[2], May Dave A.[1]

[1]*Institute of Geophysics, ETH Zurich, Sonneggstrasse 5 CH - 8092 Zurich (thomas.philippe.74@gmail.com)*
[2]*Geological Institute, ETH Zurich, Sonneggstrasse 5 CH - 8092 Zurich*

Recent fieldwork observations and numerical experiments have demonstrated that large fold-belt systems do not necessarily grow uniformly in a cylindrical manner but arise from the lateral connection (parallel to the fold axis) of smaller embryonic folds (Bretis et al., 2011). The mechanical feasibility of the linkage of two isolated embryonic folds has already been studied (Grasemann and Schmalholz 2012). In this context, the mechanical feasibility of the fork-linkage or more generally the triple-linkage (three isolated embryonic folds linking laterally together, Figure 1) is studied using the pTatin3d code1 (May et al., 2013). To address this issue, a template for modelling the triple-linkage is introduced, which consists of a solitary embryonic fold opposite to a binary perturbation.

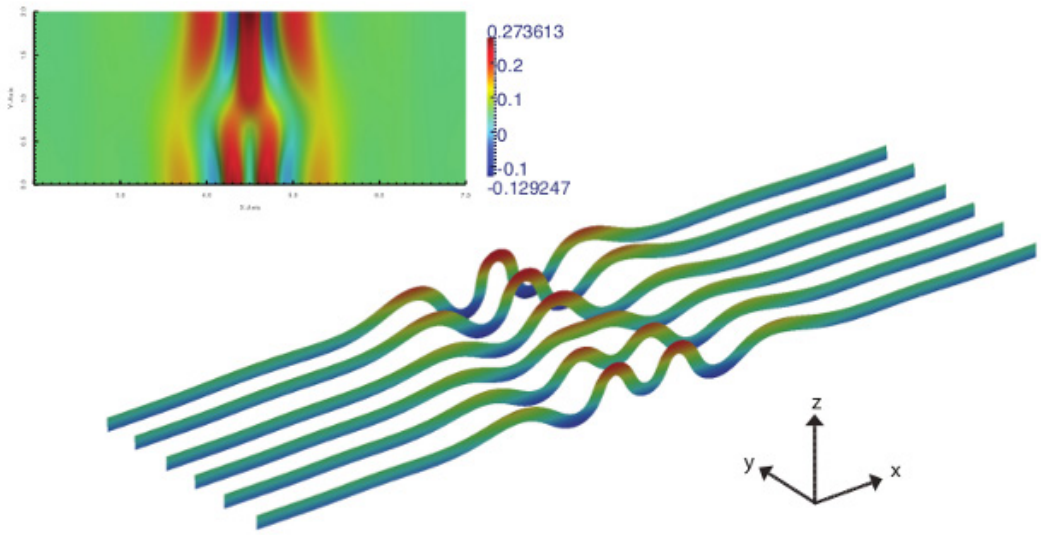

Figure 1: Triple-linkage: slices of a fork-structure. At the junction, we observe clearly a double hinge fold section with a flat topography. The colours indicate the relative topograpy.

A new terminology stemming from the observed patterns is introduced and a phase diagram highlighting the various linkage structures as a function of the geometric parameters is presented.

The folding and linkage process is tackled considering the vorticity field

$$\omega = \frac{1}{2} \nabla \times u,$$

where u is the velocity field. It turns out to be a very interesting and fruitful framework that makes the linkage patterns and embryonic fold interplays simple to understand. Based on the 3D analytical solution for the finite amplitude folding of a single viscous layer embedded in a matrix (Fletcher 1991), the planar-vorticity dominant wavelength (in the viscous layer plane) is computed numerically. This planar-vorticity dominant wavelength turns out to be distinct from the dominant amplification wavelength and it appears to be the characteristic length controlling the linkage process. In the light of these observations, a new interpretation and explanation is given for the simple-linkage previously studied and the perspectives for the general case are proposed.

[1]The pTatin3d code has been developed by D.A. May to model 3D-multiphase Stokes flows for geodynamical applications.

REFERENCES
Bretis, B., Bartl, N., and Grasemann, B. 2011. Lateral fold growth and linkage in the Zagros fold and thrust belt (Kurdistan, NE Iraq). Basin Research, 23(6), 615-630.
Fletcher, R. C. 1991. Three-dimensional folding of an embedded viscous layer in pure shear. Journal of Structural Geology, 13(1), 87-96.
Grasemann, B. and Schmalholz, S. M. 2012. Lateral fold growth and fold linkage. Geology, 40(11), 1039-1042.
May, D. A., Brown, J. and Le Pourhiet, L. 2013. A scalable, matrix-free Stokes discretisation for geodynamic applications, to be submitted to Computational Methods in Applied Mechanics and Engineering.

P 1.23

Geomorphology approach in karstic domain: importance of underground water.

Rabin Mickaël[1], Sue Christian[1], Champagnac Jean-Daniel[2] & Eichenberger Urs[3]

[*] *Chrono-environnement Laboratory, UMR 6249. University of Franche-Comté, 16 route de Gray 25000 Besançon. France (mickael.rabin@univ-fcomte.fr) (christian.sue@univ-fcomte.fr)*
[**] *Geologisches Institut. ETH-Zürich Sonneggstrasse 5 8092 Zürich. Switzerland (jean-daniel.champagnac@erdw.ethz.ch)*
[***] *ISSKA, 68 rue de la Serre CH-2301 La Chaux-de-Fonds. Switzerland (urs.eichenberger@isska.ch)*

The Jura mountain belt is the westernmost and one of the most recent expressions of the Alpine orogeny. The Jura has been well studied from a structural point of view, but still remains the source of scientific debates, especially regarding its current and recent tectonic activity [Laubscher, 1992; Burkhard et Sommaruga, 1998]. It is deemed to be always in a shortening state, according to old leveling data [Jouanne et al., 1998] and neotectonic observations on paleo-meanders of the Doubs river [Madritsch et al., 2010]. However, the few GPS data available on the Jura don't show evidence of shortening, but a small extension parallel to the arc [Walpersdorf et al., 2006]. Moreover, the traditionally accepted assumption of a collisional activity of the Jura raises the question of its geodynamic origin. The Western Alps are themselves in a post-collisional regime and characterized by a noticeable isostatic-related extension, due to the interaction between buoyancy forces and external dynamics [Sue et al., 2007].

Quantitative morphotectonic approaches are increasingly used in active mountain belt to infer relationship between climate an tectonics [Whipple, 2009]. In this study we propose to apply these tools to calcareous bedrock, in a slowly deformed mountain belt. We have used, in particular, watersheds analysis and associated rivers profiles which allow quantifying the degree and the nature of the equilibrium between the tectonic forcing and the fluvial erosional agent [Kirby and Whipple, 2001]. Slope profiles of rivers are controlled by climatic and tectonic forcing through the expression [Whipple and Tucker, 1999]:

$$S = (U / K)^{1/n} A^{m/n}$$

(with U: uplift rate, K: empirical erodibility factor, function of hydrological and geological settings; A: drained area, m, n: empirical parameters).

We present here a systematic study of these profiles applied to most of theJura rivers. First results show several abnormal signals along main rivers; for the Ain river for example, anthropogenic dams aren't always pointed, or, for the Loue river, water flow are strongly under-estimated because its spring is a karstic one. These problems are due to several factors; 1) the chemical erosion process of limestone which is, combined with classical mechanical process, more efficient and faster than erosion processes on granitic or metamorphosed bedrock, and 2) karstic losses and outlets which strongly modify water flow. The complexity of the karst system doesn't allow us to properly quantify the flow.

This study highlights the importance of underground water and the rapid chemical erosion process in a karstic domain. For further study, now we work in speleology and karstology with a structural point of view. This structural study is coupled with a morphological study of oxbows and watergap, in order to characterize the recent tectonic evolution of the Jurassian arc.

REFERENCES:
Burkhard, M. and Sommaruga, A., 1998. Evolution of the western Swiss Molasse basin: structural relations with the Alps and the Jura belt. In: Cenozoic Foreland Basins of Western Europe. (A. Mascle, C. Puidgefabregas, H. P. Luterbacher and M. Fernandez eds), Geol.Soc. Spec. Publ. 134, 279-298.
Jouanne, F., Genaudeau, N., Menard, G., Darmendrail, X., 1998. Estimating present-day displacement fields and tectonic deformation in active mountain belts: an example from the Chartreuse Massif and the southern Jura Mountains, western Alps. Tectonophysics 296, 403–419.
Kirby, E., Whipple, K., 2001. Quantifying differential rock-uplift rates via stream profile analysis. Geology 29, 415–418.
Laubscher,HP., 1992. Jura kinematics and the Molasse basin, Eclogae Geol. Helv. (85), 287-303
Madritsch, H., Fabbri, O., Hagedorn, E.-M., Preusser, F., Schmid, S.M., Ziegler, P.A., 2010. Feedback between erosion and active deformation: geomorphic constraints from the frontal Jura fold-and-thrust belt (eastern France). INTERNATIONAL JOURNAL OF EARTH SCIENCES 99, S103–S122.
Sue, C., Delacou, B., Champagnac, J.-D., Allanic, C., Tricart, P., Burkhard, M., 2007. Extensional neotectonics around the bend of the Western/Central Alps: an overview. International Journal of Earth Sciences 96, 1101–1129.
Walpersdorf, A., Baize, S., Calais, E., Tregoning, P., Nocquet, J.-M., 2006. Deformation in the Jura Mountains (France): First results from semi-permanent GPS measurements. Earth and Planetary Science Letters 245, 365–372.
Whipple, K.X., Tucker, G.E., 1999. Dynamics of the stream-power river incision model: Implications for height limits of mountain ranges, landscape response timescales, and research needs. J. Geophys. Res.-Solid Earth 104, 17661–17674.

P 1.24

The effect of hot-pressing on the grain size distribution and microstructure of quartz gouge along the brittle-to-viscous transition in shear experiments

Bettina Richter[1], Rüdiger Kilian[1], Holger Stünitz[2] & Renée Heilbronner[1]

[1] *Geological Institute, University of Basel, Bernoullistrasse 32, CH-4056 Basel (bettina.richter@unibas.ch)*
[2] *Department of Geology, University of Tromsø, Dramsveien 201, N-9037 Tromsø*

We conducted a series of shear experiments on quartz gouge in a Griggs-type solid medium deformation apparatus to investigate the brittle to viscous transition. The samples were deformed at high confining pressures of ~1.5 GPa at temperatures between 500 °C and 1000 °C at constant shear strain rates of ~5x10-5 s-1. The starting material is produced by crushing a quartz single crystal (resulting grain size <100 µm) and adding 0.2 wt% water.

First results show a decrease of the strength of the sample with increasing temperatures. Continued deformation indicates steady-state stress for the high-temperature experiments and strain hardening for lower temperatures. The grain sizes distribution of the low-temperature experiments is similar to the initial grain size distribution before deformation. With increasing temperatures the size and volume portion of the larger grains decreases while the portion of recrystallized grains increases. The crystallographic preferred orientation (CPO) of the c-axis evolves with increasing temperature from a random distribution towards (1) two elongated maxima rotated antithetically with respect to the shear sense or (2) a single y-maximum. With increasing shear strain the elongated maxima rotate with shear direction.

Some of the experiments included a hot-pressing stage (20 h at 1000 °C/~1.5 GPa) in the apparatus before the temperature was decreased to the conditions of deformation. The resulting maximum shear stresses of those experiments are significantly lower (~50 %) than those without the hot-pressing stage. In contrast, the CPO of the hot-pressed samples is similar to the samples without hot pressing at the same deformation temperature. The grain size distribution of the hot-pressed and deformed samples covers a smaller range compared to that without hot-pressing. Obviously, a size reduction of the larger grains as well as the growth of the smaller grains during the hot-pressing results in a narrower grain size distribution.

We conclude that the material with the narrower grain size distribution has a more quartzite-like behaviour, whereas the material without hot pressing behaves more like a heterogeneous fault gouge of clasts and matrix with different material properties. Thus, a fault gouge may evolve towards a homogeneous quartzite at moderate temperatures in natural rocks over extended periods of time (hot-pressing may simulate normal healing or fluid-rock interaction in nature). In addition, dynamic recrystallisation of cataclastic material or quartzite produces the same finite microstructures and we conclude that former brittle deformation can merge into plastic flow and recrystallisation.

P 1.25

Convection and grain size evolution in mantle and lithosphere of the Earth

Rozel Antoine, Tackley Paul

Institut fur Geophysic, Geophysical Fluid Dynamics, ETH Zurich, Sonnegstresse 5, 8092 Zurich

The physical mechanisms responsible for localisation of deformation in the lithosphere of the Earth remains largely misunderstood. Since very reduced grain sizes are often observed in faults and large scale shear zones, grain size is largely suspected to have an important influence on the generation of plate tectonics. Most of the grain size evolution laws derived up to now have failed to generate mature and self-sustained lithospheric shear zones in numerical computations of mantle convection. Yet, recent developments of a new physical approach of grain size reduction have shown that self-consistent plate tectonics is at hand if two-phase grain size distributions are considered instead of a single average grain size.

We present a set of numerical simulations of mantle convection including this new physical approach of two phase grain size evolution. We consider a composite rheology mixing diffusion, dislocation and grain-boundary sliding creep. This approach involving a large set of poorly constrained parameters, we only investigate the impact of grain size-dependent quantities in a reference model kept constant. Preliminary results are discussed.

P 1.26

Relationship between tectonic overpressure, deviatoric stress, driving force, isostasy and gravitational potential energy

Schmalholz Stefan[1], Medvedev Sergei[2], Lechmann Sarah[3] & Podladchikov Yuri[1]

[1] *Institut of Earth Sciences, University of Lausanne, Switzerland (stefan.schmalholz@unil.ch)*
[2] *Centre for Earth Evolution and Dynamics, University of Oslo, Norway*
[3] *Geological Institute, ETH Zurich, Switzerland; now at: armasuisse, Federal Department of Defence, Civil Protection and Sport, Switzerland*

We present analytical derivations and two-dimensional numerical simulations that quantify magnitudes of deviatoric stress and tectonic overpressure (i.e. difference between the pressure, or mean stress, and the lithostatic pressure) which arise due to variations in the gravitational potential energy (GPE). We consider a simple situation with lowlands and mountains (plateau), and a model lithosphere consisting of a crust with higher linear viscosity than the mantle. Our results (1) explain why estimates for the magnitude of stresses in Tibet, previously published by different authors, vary by a factor of two, (2) are applied to test the validity of the thin-sheet approximation, (3) show that the magnitude of the depth integrated tectonic overpressure is equal to the magnitude of the depth integrated deviatoric stress if depth integrated shear stresses within the lithosphere are negligible, and (4) show that tectonic overpressure is required to build and support continental plateaus such as in Tibet or in the Andes. The prediction of tectonic overpressure associated with GPE differences is independent of rock rheology (e.g. viscous or elastic) and rock strength. We also discuss the mechanical conditions that are necessary to achieve isostasy (i.e. the lithostatic pressure is constant) at a certain depth. The results show that tectonic overpressure can exist at a certain compensation depth although all deviatoric stresses are zero at this depth, because this tectonic overpressure is related to horizontal gradients in a force per unit length resulting from shear stresses integrated vertically across the entire lithosphere. The existence of tectonic overpressure implies that the pressure estimated from observed mineral assemblages is likely not equal to the lithostatic pressure, and pressure is not directly related to depth. However, lithostatic pressure-depth conversions, neglecting overpressure, are frequently applied in the reconstruction of the tectonic evolution of mountain ranges.

P 1.27

Exploring feldspar IRSL-50 as a low-temperature thermochronometer: insights from field applications (Alaska, Norway and Pamir)

Pierre G. Valla[1,2], Sally E. Lowick[3], Frédéric Herman[2], Jean-Daniel Champagnac[1], Benny Guralnik[1], Philippe Steer[4], Jie Chen[5] & Jintang Qin[5]

[1.] *Geological Institute, ETH Zürich, Sonneggstrasse 5, CH-8092 Zürich (pierre.valla@erdw.ethz.ch)*
[2]. *Institute of Earth Sciences, University of Lausanne, Géopolis, CH-1015 Lausanne*
[3]. *Institute of Geology, University of Bern, Baltzerstrasse 1+3, CH-3012 Bern*
[4]. *Géosciences Rennes, Université de Rennes 1, 263 Avenue du Général Leclerc, F-35700 Rennes*
[5]. *State Key Laboratory of Earthquake Dynamics, China Earthquake Administration, C-100029 Beijing*

Quartz luminescence dating has shown great potential in low-temperature thermochronometry (e.g. Herman et al., 2010) and has opened a new spatial and temporal "window" to study late stages of rock exhumation. Even though quartz OSL dating appears a suitable candidate (e.g. Li and Li, 2012), quartz separates from bedrock often show measurement complications (IR contamination, dim signals, no dateable fast component). Here, we explore feldspar IRSL-50 as an alternative signal with similar thermal characteristics, this mineral usually showing brighter signals in separates derived from bedrock. We collected samples in various mountain ranges, covering a wide range of lithologies and exhumation histories: western Norway (<0.1 mm/yr exhumation), southern Alaska (0.1-5 mm/yr exhumation), and eastern Pamir (>5 mm/yr exhumation). This offers a unique dataset to assess the potential of feldspar IRSL as a low-temperature thermochronometer.

Feldspar separates extracted from bedrock were dated using the conventional IRSL-50 protocol, which exhibits good reproducibility and dose recovery across different lithologies (although some samples may suffer from minor thermal transfer). We study fading variability in bedrock samples (using different protocols), and explore the apparent correlation between fading rate and apparent saturation ratio (e.g. Huntley and Lian, 2006). Our results show that almost all studied samples appear in field saturation (Kars et al., 2008). Indeed, feldspar saturation may limit the applicability of IRSL-50 thermochronometer to only rapidly-cooling settings (>300°C/Myr), as confirmed by isothermal holding experiments and calibration in the KTB borehole (Guralnik et al., 2010). Nonetheless, some samples from the Pamir and southern Alaska fault zones show deviation from field saturation, allowing to infer either cooling rates within rapidly-exhuming areas or localized rock reheating (through fault shearing or geothermal fluids circulation). Extending the applicability of luminescence dating in thermochronometry will require exploring lower-energy traps and/or targeting different minerals with later saturation.

REFERENCES

Herman, F., Rhodes, E.J., Braun, J. & Heiniger, L. 2010. Uniform erosion rates and relief amplitude during glacial cycles in the Southern Alps of New Zealand, as revealed from OSL-thermochronology, Earth and Planetary Science Letters, 297, 183-189.

Li, B. & Li, S.-H. 2012. Determining the cooling age using luminescence-thermochronology, Tectonophysics, 580, 242-248.

Huntley, D.J. & Lian, O.L. 2006. Some observations on tunnelling of trapped electrons in feldspars and their implications for optical dating. Quaternary Science Reviews, 25, 2503-2512.

Guralnik, B., Herman, F., Preusser, F., Rhodes, E.J., and Lowick, S.E. 2010. Preliminary constraints on the kinetics of OSL thermochronology. American Geophysical Union (AGU) Fall Meeting, San Francisco, December 2010.

P 1.28

3D FEM modelling of geological structures caused by geometrical instabilities and contrasts in rock strength

von Tscharner Marina & Schmalholz Stefan

Université de Lausanne, Institut des sciences de la Terre, Quartier UNIL-Mouline, Bâtiment Géopolis, CH-1015 Lausanne, (marina.vontscharner@unil.ch)

Many three-dimensional (3D) structures in rock, which formed during the deformation of the Earth's crust and lithosphere, are controlled by a difference in mechanical strength between rock units and are often the result of a geometrical instability. Such structures are, for example, folds, pinch-and-swell structures (due to necking) or cuspate-lobate structures (mullions).

These structures occur from the centimeter to the kilometer scale and the related deformation processes control the formation of, for example, fold-and-thrust belts and extensional sedimentary basins or the deformation of the basement-cover interface. The 2D deformation processes causing these structures are relatively well studied, however, several processes during large-strain 3D deformation are still incompletely understood. One of these 3D processes is the lateral propagation of these structures, such cusp propagation in a direction orthogonal to the shortening direction or neck propagation in direction orthogonal to the extension direction.

We study the 3D evolution of geometrical instabilities with numerical simulations based on the finite element method (FEM). Simulating geometrical instabilities caused by sharp variations of mechanical strength between rock units requires a numerical algorithm that can accurately resolve material interfaces for large differences in material properties (e.g. between limestone and shale) and for large deformations. Therefore, our FEM code combines a numerical contour-line technique and a deformable Lagrangian mesh with re-meshing. With this combined method it is possible to accurately follow the initial material contours with the FEM mesh and to accurately resolve the geometrical instabilities.

The algorithm can simulate 3D deformation for a visco-elasto-plastic rheology. Stresses are limited by a yield stress using a visco-plastic formulation and the viscous rheology is described by a power-law flow law. The 3D FEM code is applied to model 3D power-law folding and power-law Rayleigh-Taylor instabilities (diapirs) with different re-meshing scenarios. The results are tested with the analytical solution for small amplitudes and with 2D numerical results for large amplitudes.

Thereby, the small initial geometrical perturbations for folding and necking are exactly followed by the FEM mesh. In order to test and measure the numerical properties for an Eulerian mesh we use the analytical solution for a two-dimensional viscous inclusion in pure shear.

P 1.29

Slab detachment – 3D versus 1D

von Tscharner Marina, Duretz Thibault & Schmalholz Stefan

Université de Lausanne, Institut dessciences de la Terre, Quartier UNIL-Mouline, Bâtiment Géopolis, CH-1015 Lausanne, (marina.vontscharner@unil.ch)

Slab detachment is ageodynamic mechanism that may affect subduction zones on Earth. The model is characterized by the detachment of a subducting slab fragment and results in a dramatic decrease of the slab pull force magnitude. As a result, slab detachment has many potential consequences for the dynamics of convergent zones such as orogens.

We study three-dimensional (3D) lateral propagation of slab detachment with a lateral varying initial slab length with numerical simulations based on the finite element method (FEM). The slab detachment is simulatedby buoyancy-driven necking in a layer of power-law fluid embedded in a linear viscous medium. Our 3D FEM code combines a numerical contour-line technique and a deformable Lagrangian mesh with re-meshing. With this combined method it is possible to accurately follow the initial material contours with the FEM mesh and to accurately resolve the geometrical instabilities. We are able to follow the material contour and therefore, to study the accurate slab geometry at any time.

We provide a detailed description of the evolution of the slab morphology and evaluate the rates of lateral propagation of slab detachment.
We compare the 3D results with the one dimensional (1D) necking analytical solution by Schmalholz (2011). The numerical results give reasonably good agreement with the analytical prediction, despite the fact that 3D detachment may occur on a much longer timescale.

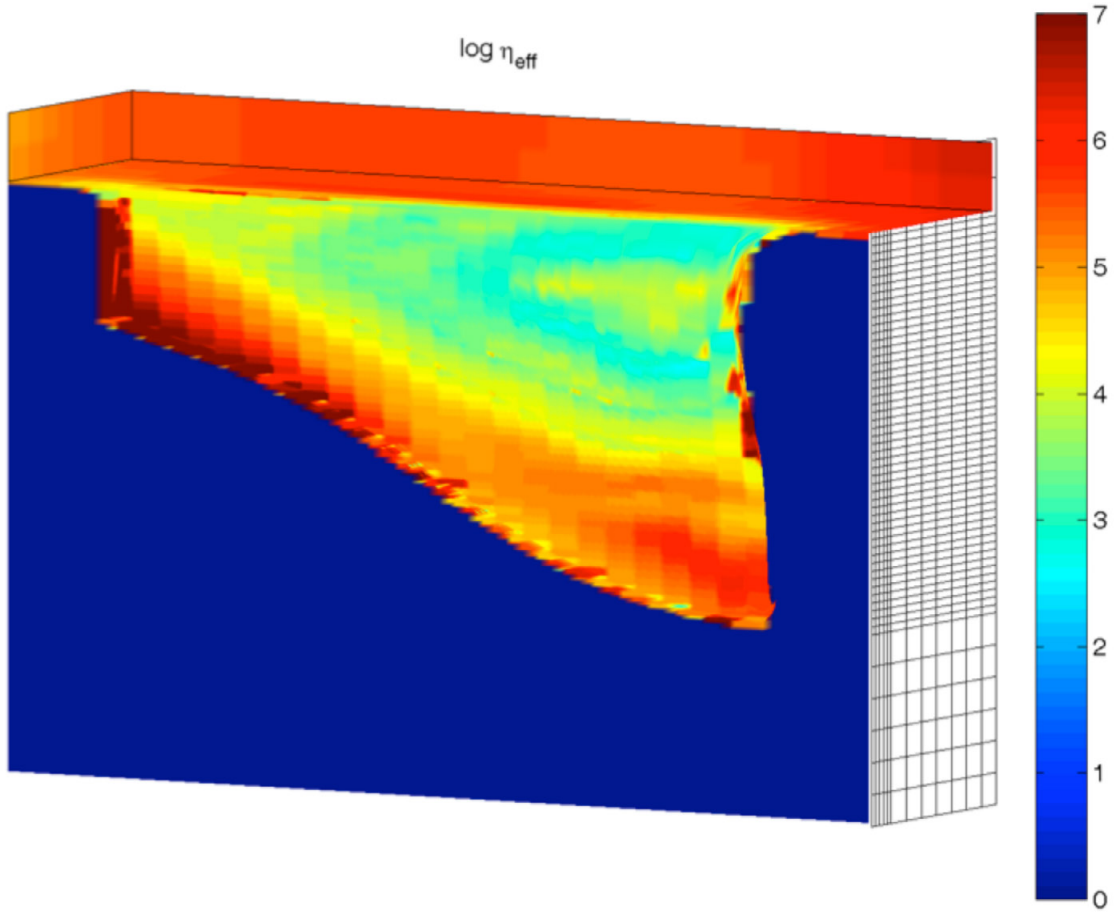

Figure 1: color plot of effective viscosity on the slab contour.

REFERENCES

Schmalholz, S., 2011, A simple analytical solution for slab detachment, Earth and Planetary Science Letters 304, 45-54

P 1.30

Baijiantan-Baikouquan ophiolitic mélanges: Implications for geology evolution of west Junggar, Xinjiang, NW China

Zhu Y.F.

The Key Laboratory of Orogenic Belts and Crustal Evolution, Ministry of Education, China; School of Earth and Space Science, Peking University, Beijing 100871, China

The west Junggar, as a major component of the core part of the central Asian Orogenic Belt, is considered to be a Paleozoic orogenic belt resulting from the convergence of the Siberian and Kazakhstan-Junggar plates. Three ophiolite belts occur in this region (Fig. 1): the Tangbale ophiolite mélange in west; the Darbut-Sartohay ophiolite mélanges in northeast, and the newly discovered Baijiantan-Baikouquan ophiolitic mélanges in southeast (Feng, 1986; Zhang, 1997; Chen & Zhu, 2011; Zhu et al. 2011). This paper focuses on petrology and geochemistry of the Baijiantan-Baikouquan ophiolite mélanges. We provide the comprehensive geologic, petrographic, and geochemical data-set, discuss the P-T conditions for the metamorphic evolution of the ophiolitic mélanges based on thermodynamically calculated P-T pseudosections for garnet amphibolite, and interpret the lithological characteristics of the west Junggar in a subduction-accretion scheme.

Lherzolite consists mainly of olivine, orthopyroxene, clinopyroxene, spinel and serpentine. Brown spinel with homogeneous composition were replaced by ilmenite along rim. Metagabbro consists of clinopyroxene, plagioclase pseudomorph, amphibole, and other second mineral phases. Plagioclase occurs as pseudomorph consisting mainly of zoisite and albite. Clinopyroxene, as a mineral phase crystallized from magma, was replaced by amphibole along rim. Garnet occurs along the rim of plagioclase pseudomorph. This suggests a transformation from plagioclase to garnet, which was accompanied with chlorite and ilmenite. Garnet amphibolite contains various amounts of garnet and amphibole with minor amounts of zoisite, epidote, chlorite, clinopyroxene, ilmenite, biotite, and sphene. Garnet contains various kinds of mineral inclusions including clinopyroxene, rutile, apatite, ilmenite, biotite, and quartz. All garnet analyses fall in the field corresponding to the garnet in eclogite coexisting with bluschist.

Zircon SHRIMP analyses give a weighted average U-Pb age of 385.0 ±3.3Ma for metagabbro and 363.3 ±3.1Ma for amphibolite. We consider the U-Pb age of ~385Ma could most probably represent the magma intrusion time, while the younger age might be affected by metamorphism.

Two Ordovician ophiolitic belts could be identified in west Junggar: the TTKH locating on the south boundary of the Chingiz-Tarbahatai arc, and the TBB locating on the south of west Junggar (Fig. 1). The Darbut–Sartohay ophiolitic belt, occurring between the above two Ordovician ophiolitic belts, was formed during Devonian. The TTKH represents an accretionary terrane added on the south edge of Chingiz-Tarbahatai arc, which was intruded by Silurian granitic rocks. The TBB represents an accretionary terrane added on the Junggar plate. The Darbut–Sartohay ophiolitic belt represents the relics of the Paleo-Ocean floor. The lithologic units of the TBB and Darbut–Sartohay ophiolitic mélanges were intruded by Carboniferous granite.

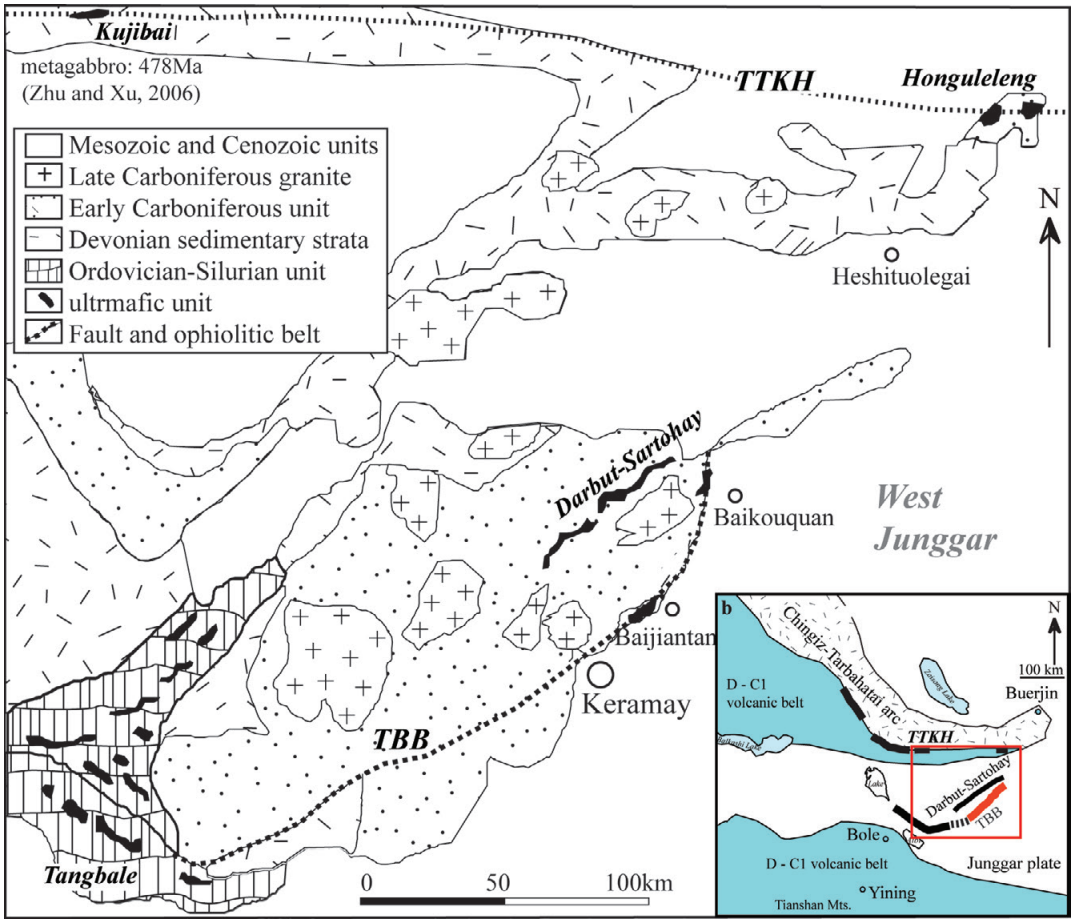

Figure 1. Simplified geological map showing the major geological units and the distribution of ophiolite belts in west Junggar.

REFERENCES

Chen, B. & Zhu, Y.F. 2011: Petrology, geochemistry and zircon U-Pb chronology of gabbro in Darbut ophiolitic melange, Xinjiang. Acta Petrologica Sinica, 27, 1746-1758.

Feng, Y. M. 1986: Genetic environments and original types of ophiolites in west Junggar. Bull. Xi'an Inst. Geol. Min. Res., Chinese Acad. Geol. Sci., 13, 37-45.

Zhang, L.F. 1997: 40Ar/39Ar age of blueschists in Tangbale, western Junggar, Xinjiang, and its significance. Chinese Science Bulletin, 42, 2178-2181.

Zhu, Y.F. & Xu, X. 2006: The discovery of Early Ordovician ophiolite mélange in Tarbahatai Mts., Xinjiang, NW China. Acta Petrologica Sinica, 22, 2833-2842.

Zhu, Y.F., Yan, Q.M., Ma, H.D. & Lehmann, B. 2011: Recent advances in geology and exploration in the Balkash-western Junggar region (Kazakhstan and Xinjiang, China): Report on the "International workshop on the large Balkash-western Junggar copper-gold province", Karamay, Xinjiang, China, 22-27 August, 2011. Episodes, 34, 208-211.